Molecular Phylogenetics and Evolution 180 (2023) 107707

Contents lists available at ScienceDirect

Molecular Phylogenetics and Evolution

journal homepage: www.elsevier.com/locate/ympev

Expanding *Acutuncus*: Phylogenetics and morphological analyses reveal a considerably wider distribution for this tardigrade genus

Matteo Vecchi [a,*], Alexandra Tsvetkova [b], Daniel Stec [c], Claudio Ferrari [d], Sara Calhim [a], Denis Tumanov [b,e,*]

[a] Department of Biological and Environmental Science, University of Jyvaskyla, PO Box 35, FI-40014 Jyvaskyla, Finland
[b] Department of Invertebrate Zoology, Faculty of Biology, Saint Petersburg State University, 199034, Universitetskaya nab. 7/9, Saint Petersburg, Russia
[c] Institute of Systematics and Evolution of Animals, Polish Academy of Sciences, Sławkowska 17, 31-016 Kraków, Poland
[d] Department of Chemistry, Life Sciences and Environmental Sustainability, University of Parma, Parco Area delle Scienze 33/A, 43124 Parma, Italy
[e] Zoological Institute of the Russian Academy of Sciences, 199034, Universitetskaja nab. 1, Saint Petersburg, Russia

ARTICLE INFO

Keywords:
Tardigrade
Antarctica
Integrative taxonomy
Endemism
Polar region

ABSTRACT

The tardigrade genus *Acutuncus* has been long thought to be an Antarctic endemism, well adapted to this harsh environment. The Antarctic endemicity of *Acutuncus* was recently dispelled with the description of *Acutuncus mariae* Zawierucha, 2020 found in the Svalbard archipelago. The integrated analyses on two newly found *Acutuncus* populations from UK and Italy, and a population of *Acutuncus antarcticus* found close to its type locality allowed us to expand the climatic and geographic range of the genus *Acutuncus*. These findings also allowed us to re-evaluate the morphological diagnoses of *Acutuncus* and accommodate it in the newly proposed monotypic family Acutuncidae **fam. nov.** Two new *Acutuncus* species morpho-groups are instituted based on eggs morphology: one (*Acutuncus antarcticus* morphogroup) including the Antarctic *Acutuncus* taxa characterized by eggs with long pillars within the chorion and eggs laid freely to the environment, the other (*Acutuncus mariae* morphogroup) including the European species, characterized by eggs with short pillars within the chorion and eggs laid in the exuvium. Finally, we describe two new *Acutuncus* species from Europe: *Acutuncus mecnuffi* **sp. nov.** and *Acutuncus giovanniniae* **sp. nov.**

1. Introduction

Tardigrades are a phylum of microscopic metazoans living in freshwater, marine and limno-terrestrial environments throughout the world (Schill, 2019). Since the first species description in 1834 (Schultze, 1834), more than 1400 tardigrade species are recognized within the phylum (Guidetti and Bertolani, 2005; Degma and Guidetti, 2007; Degma and Guidetti, 2022). Until relatively recently, the systematics and taxonomy of tardigrades has been predominantly based on morphology. In the last several years, however, the advent of molecular techniques has allowed us to clarify relationships that were impossible to uncover by morphology alone (Cesari et al., 2016b; Tumanov, 2020a,2022; Stec et al., 2020a; Stec and Morek, 2022; Zawierucha et al., 2022). Despite having a clear idea of the evolutionary relationships between the Eutardigrada superfamilies and especially of the most common taxa (Bertolani et al. 2014), some rarer and less conspicuous taxa still evade a precise phylogenetic placement and defined morphological diagnosis, e.g., *Acutuncus*, a genus in the superfamily Hypsibioidea.

Acutuncus (Pilato and Binda, 1997) is a genus with a long and complicated history. Since its type species *Macrobiotus antarcticus* (Richters, 1904) was described from Antarctica, numerous misidentifications fostered by its unclear initial description were recorded from all around the world (Dastych, 1991). Almost 90 years after its description, Dastych (1991) presented a thorough review of the type material and records that had been assigned to this species over the years, provided a clear morphological description of this species as *Hypsibius antarcticus* (Richters, 1904), and revealed that the only valid

Abbreviations: AISM, apophyses for the insertion of the stylet muscles; DIC, differential interference contrast microscopy; PhC, phase contrast microscopy; SEM, Scanning Electron Microscopy; SPbU, Saint Petersburg State University; JYU, University of Jyvaskyla.

* Corresponding authors at: 199034, Universitetskaya nab. 7/9, Saint Petersburg, Russia (D.V. Tumanov). Department of Biological and Environmental Science, University of Jyvaskyla, PO Box 35, FI-40014 Jyvaskyla, Finland (M. Vecchi).

E-mail addresses: matteo.vecchi15@gmail.com (M. Vecchi), d.tumanov@spbu.ru (D. Tumanov).

https://doi.org/10.1016/j.ympev.2023.107707
Received 15 October 2022; Received in revised form 11 January 2023; Accepted 12 January 2023
Available online 18 January 2023

records belonged to Antarctica. The monotypic genus was then erected by Pilato and Binda (1997) based on the presence of both *Hypsibius* and *Isohypsibius* type claws (a character shared with the genus *Mixibius*; Pilato, 1992), the apophyses for the insertion of the stylet muscles in the shape of sharp hooks, and the presence of freely laid eggs with an ornamented chorion. The affinity of *Acutuncus* to *Hypsibius* and related genera has never been questioned, and molecular analyses (Bertolani et al. 2014) confirmed it belonged to the family Hypsibiidae. However, the position within the family was not crystal clear, which led to its placement as *incerta subfamilia*. *Acutuncus* has been considered an Antarctic endemic since 1997 (with only three dubious records in Argentina and Colombia, see Kaczmarek et al., 2015 and references therein).

Notably a new species, *Acutuncus mariae* Zawierucha, 2020 was recently described from cryoconites holes in the Svalbard Islands (Zawierucha et al. 2020), expanding the geographic range of the genus. Van Rompu & De Smet (1991) also reported one *Acutuncus* (as *Hypsibius antarcticus*) individual from a freshwater pond in the Svalbard archipelago. Only drawings of the animals, but without microphotographs or data on egg morphology, were presented precluding the possibility to confirm this record and assign it to *A. mariae*.

Recently, *Acutuncus* was also reported from Norway (Topstad et al., 2021) only based on molecular data (a 383 base pairs fragment of the SSU gene). This finding was already flagged as dubious by the authors (Topstad et al., 2021) due to a low genetic distance threshold for assigning a positive match (98%) and the absence of *Acutuncus* from the individuals identified by morphology. In the present study, the discovery of two new tardigrade species affiliated with *Acutuncus* led us to perform a re-examination of the definition for the genus *Acutuncus* and its composition. Using extensive phylogenetic analysis and detailed morphological investigation we accommodated *Acutuncus* into a new eutardigrade family Acutuncidae **fam. nov.**, also dividing its members into two morphogroups differing in egg chorion morphology, and egg laying strategy.

2. Materials and methods

2.1. Samples and specimens

Information on samples of algae, rock pool, and gutter sediments analysed in this study are provided in Table 1. Tardigrades were extracted from fresh and frozen samples by washing them through two sieves (Tumanov, 2018). The content of the fine sieve was examined under a Leica M205C stereo microscope. To perform the taxonomic analysis, animals and eggs were divided into several groups for specific analyses: morphological analysis with PhC and SEM, as well as DNA sequencing. Additional data (morphological and morphometric) were gathered from photographs and measurements present in species descriptions or kindly provided by our colleagues (Table 2).

Table 2
Additional comparative material examined.

Taxa	Locality	Type material (Y/N)	Source
Acutuncus mariae Zawierucha, 2020	Svalbard, Norway	Y	Zawierucha et al. (2020)
Acutuncus antarcticus (Richters, 1904)	West Ongul Island, Antarctica	N	Kagoshima et al. (2013)

2.2. Microscopy and imaging

Tardigrades were fixed with acetic acid or relaxed by incubating live individuals at 60 °C for 30 min and mounted on slides in Hoyer's medium (Morek et al. 2016). Permanent slides were examined under a Leica DM2500 microscope equipped with phase contrast (PhC) and differential interference contrast (DIC). Photographs were made using a Nikon DS-Fi3 digital camera with NIS software.

For scanning electron microscopy (SEM), the protocol from Tumanov (2020a) was used. Specimens and eggs were dehydrated in an ascending ethyl alcohol series (10%, 20%, 30%, 50%, 70%, 96%) and acetone or 100% ethyl alcohol, critical point dried in CO_2, mounted on stubs, and coated with gold. A Tescan MIRA3 LMU (Centre for Molecular and Cell Technologies, St. Petersburg State University) and a Raith e-LiNE (Nanoscience Center, University of Jyväskylä) scanning electron microscopes were used for observations.

2.3. Morphometrics and terminology

All measurements are given in micrometres (μm). Structures were measured only if their orientation was suitable. Body length was measured from the anterior end of the body to the posterior end, excluding the hind legs. The buccal tube was measured from the anterior margin of the stylet sheaths to the caudal end of the buccal tube, excluding the buccal apophyses. Terminology for the structures within the buccopharyngeal apparatus and for the claws follows Pilato and Binda (2010). Elements of the buccal apparatus were measured according to Kaczmarek and Michalczyk (2017). Claws were measured following Beasley et al. (2008), but the total length of the claws was also measured (according to Pilato et al. 2002) to ensure compatibility with older publications. Also, recently introduced indexes were calculated for the claws' length. The first index used here is the base:primary branch ratio given as a percent, and presented under the name "*cct*" (claw common tract) in Tardigrada Register "Parachela" template 1.8 (Michalczyk and Kaczmarek, 2013). This index was initially introduced for Macrobiotoidea by Guidetti et al. (2016) as base:primary branch length ratio, with the primary branch length measured according to Pilato et al. (2002) (i.e., measured from the base of the basal part to the tip of the primary branch, corresponding to the claw total length). However, in Hypsibioidea/Isohypsibioidea the primary claws branch

Table 1
Examined species along with their sampling details and number of specimens used. Individual numbers are expressed as number of tardigrades (T) and number of eggs (E) analysed.

Species	Sample code - institution	Locality	Coordinates	Substrate	Collection date	Collector	Inds. analyzed for morphology and/or morphometry	Inds. sequenced
Acutuncus antarcticus (Richters, 1904)	286 - SPbU	Haswell Island, Antarctica	approx. −66.525757, 92.995123	Algae on soil	03.01.2014	Boris Anohin	101 T + 21 E	3 T
Acutuncus giovanniniae sp. nov.	S283 - JYU	Parma, Italy	44.387421 10.020868	Pothole sediment	24/06/2020	Matteo Vecchi and Claudio Ferrari	68 T + 37 E	6 T (COI sequences already published in Vecchi et al., 2022)
Acutuncus mecnuffi sp. nov.	S426 -JYU	Manchester, UK	NA	Gutter sediment	2017	Bob McNuff	136 T + 29 E	2 T

lengths used to calculate the ratio with the base are usually measured according to Beasley et al. (2008). This different measuring methods, used preferentially for different Parachela taxa lead to having two effectively different indexes under one name. To avoid misunderstandings, we propose to keep using the "*cct*" terminology when the primary branch lengths based on the index calculation following Pilato et al. (2002), whereas we propose to use "*cbt*" (claw basal tract) as new name for the base:primary branch ratio when the primary branch length is measured according to Beasley et al. (2008). The second index is the "*br*" ratio, i.e., the ratio of the height of the secondary claw branch to the height of the primary claw branch (Gąsiorek et al., 2019), given here as a percentage. The *pt* index used is the percentage ratio between the length of a structure and the length of the buccal tube (Pilato, 1981) and is presented here in italics. Morphometric data were handled using ver. 1.8 of the "Parachela" template, which is available from the Tardigrada Register (Michalczyk and Kaczmarek, 2013) with addition of the total length of the claws.

2.4. Genotyping

The DNA extraction, amplification and sequencing was performed in two different laboratories with different instrumentation and reagents availability; thus, two slightly different protocols were used. For the *Acutuncus antarcticus* specimens, DNA was extracted from a single specimen using QuickExtractTM DNA Extraction Solution (Lucigen Corporation, USA, see complete protocol description in Tumanov, 2020b). Fragments of four genes were sequenced: a small ribosome subunit (18S rRNA) gene, a large ribosome subunit (28S rRNA) gene, internal transcribed spacer (ITS-2), and the cytochrome oxidase subunit I (COI) gene. PCR reactions included 5 μl template DNA, 1 μl of each primer, 1 μl DNTP, 5 μl Taq Buffer (10X) (-Mg), 4 μl 25 mM $MgCl_2$ and 0.2 μl Taq DNA Polymerase (Thermo Scientific™) in a final volume of 50 μl. The primers and PCR programs used are provided in Supplementary Material SM.01. The PCR products were visualized in 1.5% agarose gel stained with ethidium bromide. All amplicons were sequenced directly using the ABI PRISM Big Dye Terminator Cycle Sequencing Kit (Applied Biosystems, Foster City, CA, USA) with the help of an ABI Prism 310 Genetic Analyzer in the Core Facilities Center "Centre for Molecular and Cell Technologies" of St Petersburg State University. The DNA from specimens from samples S283-JYU and S426-JYU were extracted, the respective fragments amplified and sequenced according to the protocols and with primers used in Stec et al. (2020b). These sequencing products were read with the ABI Prism 310 Genetic Analyzer at the Institute of Systematics and Evolution of Animals, Polish Academy of Sciences, Kraków, Poland. Sequences were edited and assembled using ChromasPro software (Technelysium, USA). The COI sequences were translated to amino acids using the invertebrate mitochondrial code, implemented in MEGA7 (Kumar et al. 2016), to check for the presence of stop codons and therefore of pseudogenes.

2.5. Phylogenetic analysis and species delimitation

Two phylogenetic trees were produced: one based on the concatenated 18S and 28S rRNAs (spanning all Hypsibioidea) and one based on the COI marker (only for *Acutuncus*). GenBank accession numbers of all sequences used in the analysis are given in Supplementary Material SM.02. The COI and ITS-2 markers were not included into the analysis because the inclusion of fast-evolving genes may negatively affect the resolution of deep phylogenetic relationships (Betancur et al., 2014; Chen et al., 2015; Klopfstein et al., 2017; Tumanov 2022).

For the 18S + 28S tree, representative of Hypsibioidea (with members of Ramazzottidae and *Pseudobiotus megalonyx* (Thulin, 1928) as outgroup) were chosen based on the presence of overlapping 18S and 28S sequences with those newly produced in this study. The sequences were aligned using MAFFT ver. 7 (Katoh et al. 2002; Katoh and Toh, 2008) with the G-INS-i method (thread = 4, threadtb = 5, threadit = 0, reorder, adjust direction, any symbol, max iterate = 1000, retree 1, global pair input) and concatenated with the R package "concatipede" (Vecchi and Bruneaux, 2021). Model selection and phylogenetic reconstructions were undertaken using the CIPRES Science Gateway (Miller et al. 2010). Model selection was performed for each alignment partition using PartitionFinder2 (Lanfear et al. 2016). Bayesian inference (BI) phylogenetic reconstruction was performed using MrBayes v3.2.6 (Ronquist et al. 2012) without BEAGLE. Two runs (one cold chain and three heated chains each) of 20 million generations were used with a burn-in of 2 million generations, sampling a tree every 1000 generations. Posterior distribution sanity was checked using Tracer v1.7 (Rambaut et al. 2018). As the tree was poorly resolved, a Rogue taxa analysis was performed based on Leaf Stability with RogueNarock online server (Aberer et al. 2013). From the collection of tree posteriors, the taxa identified as rogue (with a leaf stability score lower than the outgroups) were removed and the consensus tree recalculated. The script and intermediate results for performing the rogue taxa analysis are available as Supplementary materials SM.03-04-05. The phylogenetic tree was visualized with the R package "phytools" (Revell, 2012) and the image was edited with Inkscape 0.92.3 (Bah, 2011).

Maximum-likelihood (ML) topology was constructed for the same dataset (with "rogue taxa" removed) using IQ-TREE multicore version 1.6.12 (Kalyaanamoorthy et al., 2017; Minh et al., 2020).

For the COI tree, all sequences from GenBank attributed to *Acutuncus* (with *Hypsibius exemplaris* Gąsiorek, Stec, Morek and Michalczyk, 2018 as outgroup) were used in the phylogenetic reconstruction. The sequences were aligned according to their amino acid sequences (translated using the invertebrate mitochondrial code) with the MUSCLE algorithm (Edgar, 2004) in MEGA7 with default settings (i.e., all gap penalties = 0, max iterations = 8, clustering method = UPGMB, lambda = 24). Alignments were visually inspected and trimmed in MEGA7. Model selection was performed for each alignment partition using PartitionFinder2 (Lanfear et al. 2016). Bayesian inference (BI) phylogenetic reconstruction was performed using MrBayes v3.2.6 (Ronquist et al. 2012) without BEAGLE. Two runs (one cold chain and three heated chains each) of 20 million generations were used with a burn-in of 2 million generations, sampling a tree every 1000 generations. Posterior distribution sanity was checked using Tracer v1.7 (Rambaut et al. 2018). The phylogenetic tree was visualized with FigTree v1.4.4 (Rambaut, 2007), and the image was edited with Inkscape 0.92.3 (Bah, 2011).

Maximum-likelihood (ML) topology was constructed for the same dataset using IQ-TREE multicore version 1.6.12 (Kalyaanamoorthy et al., 2017; Minh et al., 2020).

Species delimitation was done on the same COI alignment used for the COI phylogenetic reconstruction in the ASAP online server (Puillandre et al. 2021) and bPTP (Zhang et al. 2013).

All partitions and model selection results are contained in Supplementary Materials (SM.06).

The MrBayes input files with the input alignments are available as Supplementary Materials (SM.07-08), and the MrBayes output consensus trees are available as Supplementary Materials (SM.09-10). Maximum-likelihood output consensus trees are available as Supplementary Materials (SM.11-12) Species delimitation with ASAP and bPTP results are available as Supplementary Materials (SM.13).

3. Results

3.1. Phylogenetic analysis

3.1.1. SSU and LSU Hypsibioidea phylogeny

The Bayesian phylogenetic reconstruction based on the ribosomal markers (Fig. 1) recovered all currently recognized families and subfamilies of Hypsibioidea (Degma and Guidetti, 2022) as monophyletic, with the exceptions of Calohypsibiidae and Pilatobiinae. Four terminals (*Pilatobius ramazzottii* (Robotti, 1970), *Mixibius saracenus*, *Mixibius* cf. *saracenus*, *Calohypsibius ornatus* 1) were recognized to be "rogue taxa" by

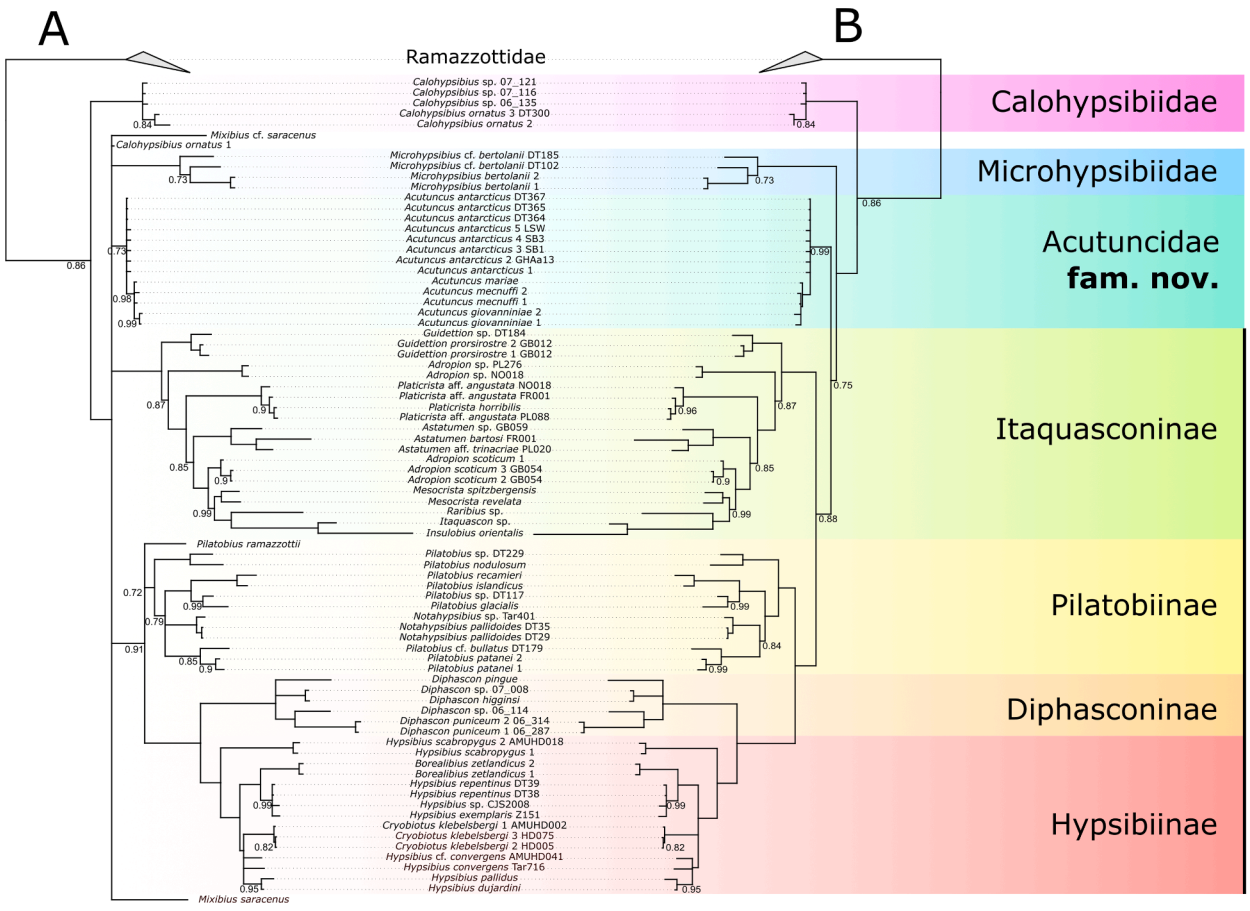

Fig. 1. BI Phylogenetic tree of Hypsibioidea based on concatenated SSU and LSU markers. A) Phylogenetic tree with rogue taxa; B) Phylogenetic tree without rogue taxa. Outgroup (*Pseudobiotus megalonyx*) not shown. Nodes with posterior probability (pp) < 0.70 were collapsed. Numbers below branches indicate pp. Nodes without numbers have pp = 1.

leaf stability analysis (SM.05), and when the consensus tree from the posterior distribution of trees was computed after their removal, the general topology was maintained but with generally higher support values and with the monophyly of all families and subfamilies recovered (Fig. 1). Additionally, in both trees, all members of the genus *Acutuncus* form a monophyletic clade clearly separated and not belonging to any other family or subfamily. The newly described species (*Acutuncus giovanniniae* **sp. nov.** and *Acutuncus mecnuffi* **sp. nov.**, see taxonomic

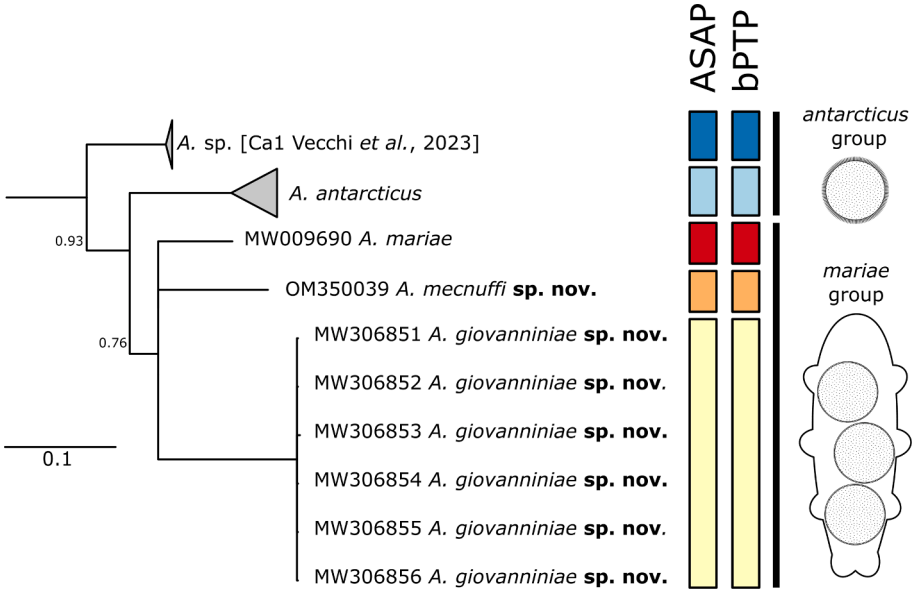

Fig. 2. Phylogenetic tree of *Acutuncus* based on COI, results of species delimitation analyses, and schematic representation of egg morphology in the two subgenera. Nodes with posterior probability (pp) < 0.70 were collapsed. Numbers below branches indicate pp. Nodes without numbers have pp = 1.

account section for details), are clearly phylogenetically affiliated with other *Acutuncus*.

The Maximum-likelihood phylogenetic reconstruction based on the same dataset recovered the same tree topology (SM.11) with high support values (bootstrap values 99–100%) for all currently recognized families and subfamilies of Hypsibioidea. Similarly, as in Bayesian reconstruction, also here all members of the genus *Acutuncus* form a clearly separated monophyletic clade, which does not belong to any other family or subfamily.

3.1.2. COI phylogeny and species delimitation

The phylogenetic reconstruction based on the COI marker (Fig. 2) recovered two clades of sequences attributed to Antarctic taxa of the genus *Acutuncus* forming a paraphyletic group. Sequences of *A. mariae* and the two new examined species formed a weakly supported (0.76 posterior probability) monophyletic group and are monophyletic with respect to each other. Both species delimitation methods (ABGD and bPTP) recovered the five identified clades (two clade of Antarctic *Acutuncus, A. mariae* and the two new species) as separate and distinct species. Results of the Maximum-likelihood phylogenetic reconstruction based on the same dataset recovered the same tree topology (SM.12).

4. Discussion

4.1. Acutuncus distribution and biogeography

After the initial description from East Antarctica (Richters, 1904), *A. antarcticus* was recorded not only from the Antarctic region, but also from the northern hemisphere. These records were usually based on a small number of individuals and did not include a detailed morphological description (see Dastych, 1991 for review). The problem of the correct identification of the material collected from outside Antarctica is exacerbated by the presence of another poorly described Arctic species with similar eggshell morphology – *Hypsibius arcticus* (Murray, 1907b). Dastych (1991) redescribed *A. antarcticus* based on Richter's type material and considered only Antarctic records of this species to be credible. He also suggested that Antarctic records of *H. arcticus* could in fact be treated as records of *A. antarcticus* (Dastych, 1991). The taxonomical uncertainty regarding identification of *H. arcticus* and *A. antarcticus* from the north hemisphere were left unresolved at that time.

About two decades later, the genetic diversity of Antarctic populations of *A. antarcticus* was studied using the comparative analysis of the COI gene sequences (Czechowski et al. 2012; Kagoshima et al. 2013; Cesari et al. 2016a). It was shown that, although a complex of similar COI haplotypes is widely distributed over all the Antarctic continent, at least one markedly different population (Sør Rondane Mountains, Czechowski et al. 2012) was present. Unfortunately, no morphological data are available for this population. The existence of populations with genetic *p*-distances of 19.2–20.8% is considered as evidence of cryptic speciation within Antarctic *Acutuncus* (Cesari et al. 2016a). This hypothesis is supported by the results of the current phylogenetic analysis (Fig. 2) and morphological data obtained during our investigation (although the great morphological variability of *A. antarcticus* populations was also mentioned previously (Dastych, 1991; McInnes, 1995). Based on the phylogenetic placement of the *A. antarcticus* sequences from Haswell Island, one of the two Antarctic *Acutuncus* species is assigned to *A. antarcticus* (Fig. 2), whereas the other one is considered as an unconfirmed candidate species (UCS; Padial et al. 2010) and defined as *Acutuncus* sp. [Ca. 1 Vecchi et al., 2023].

Recently, Zawierucha et al. (2020) described a new species of the genus *Acutuncus* from the Svalbard archipelago: *A. mariae*. It is the first *Acutuncus* species reported from the northern hemisphere, with its' taxonomic position supported by gene sequence data combined with detailed morphological data on both adult animals and eggs. This finding, together with two new *Acutuncus* species described in the present study, indicates the existence of the clade of *Acutuncus*-like organisms with a distribution that is not limited to the Antarctic region.

The species *H. arcticus* was transferred by Gąsiorek et al. (2018) to the genus *Ramazzottius* based on the description of *Ramazzottius*-like claws and free laid eggs. This proposal was later contested by Tumanov (2020a) who transferred *H. arcticus* to the newly described genus *Notahypsibius* Tumanov (2020a) that comprises species with *Acutuncus*-like eggshell structures. The newly discovered diversity of European *Acutuncus* species makes it more likely that the species described from Franz Joseph Land as *H. arcticus*, as well as a poorly described form from Scotland (Murray, 1907a), both belong to the genus *Acutuncus*.

4.2. Updated description of Acutuncus antarcticus

Since Richters (1904) description of *A. antarcticus*, no material has been collected from the type locality (Gaussberg region). All currently available gene sequences attributed to *A. antarcticus* are derived from specimens collected from other Antarctic locations far from the type locality of this species. Considering that Haswell Island seems to be the closest site of the exposed earth surface to the Gaussberg region (171 km, measured using Google Earth©), the collection and sequencing of a population of *A. antarcticus* from this locality gave us the opportunity to pinpoint which of the two *Acutuncus* clades, found by phylogenetic analysis and species delimitation, could be assigned to *A. antarcticus*. Also, the morphological similarity of our specimens to Richter's material (Dastych, 1991) provide evidence that the Haswell Island population is correctly identified as *A. antarcticus*. The large number of specimens collected, and the sequences obtained for all four phylogenetically significant genes, gives us a chance to make a detailed integrative description of the Haswell Island population of *A. antarcticus*.

5. Taxonomic account

Phylum: Tardigrada Doyère, 1840.

Class: Eutardigrada Richters, 1926.

Order: Parachela Schuster et al. 1980 (restored by Morek et al. 2020).

Superfamily: Hypsibioidea Pilato, 1969 in Marley et al. 2011.

Family: Acutuncidae fam. nov. Vecchi, Tsvetkova, Stec, Ferrari, Calhim, Tumanov 2023.

urn:lsid:zoobank.org:act:E284745E-BE96-4408-8328-AAA0343142A1.

AISMs in form of hooks, asymmetrical with respect to the frontal plane with dorsal hook being shorter and higher than the ventral. Caudal ends of AISMs usually blunt or round, not forming obviously sharp points. Dorsal and ventral thickenings of the buccal tube posterior to the AISMs, present. Pharynx with two macroplacoids, without microplacoids or septulum. External claws of the *Isohypsibius* type, internal claw of the *Hypsibius* type (Pilato & Binda, 2010). Eggs with pillars in the chorion, visible under LM.

Composition: *Acutuncus* Pilato and Binda, 1997.

Genus: *Acutuncus* Pilato and Binda, 1997 (emended)

The same characters as for the family.

Type species: *Acutuncus antarcticus* (Richters, 1904)

Updated description of *Acutuncus antarcticus*.

Material studied. 101 specimens and 21 eggs (78 specimens and 16 eggs on slides mounted in Hoyer's medium and 23 specimens and 5 eggs on SEM stubs). Sex indet.; Haswell Island, East Antarctica, approx. −66.525757, 92.995123, algae on soil, 03.01.2014, Boris Anohin leg.; Slides SPbU 286(1)–286(20) deposited at St. Petersburg State University.

Animals. Body small, elongate, slightly widened at the level of legs III (Fig. 3A, 4A), with a blunt snout (for comparison see the sharp snout of *Itaquascon*) (morphometrics: Table 3 and Supplementary material SM.14). Body transparent or whitish. With large eyespots visible in preserved specimens (Fig. 3A). Cuticle smooth (Fig. 4A).

Mouth opening anteroventral, on developed mouth cone;

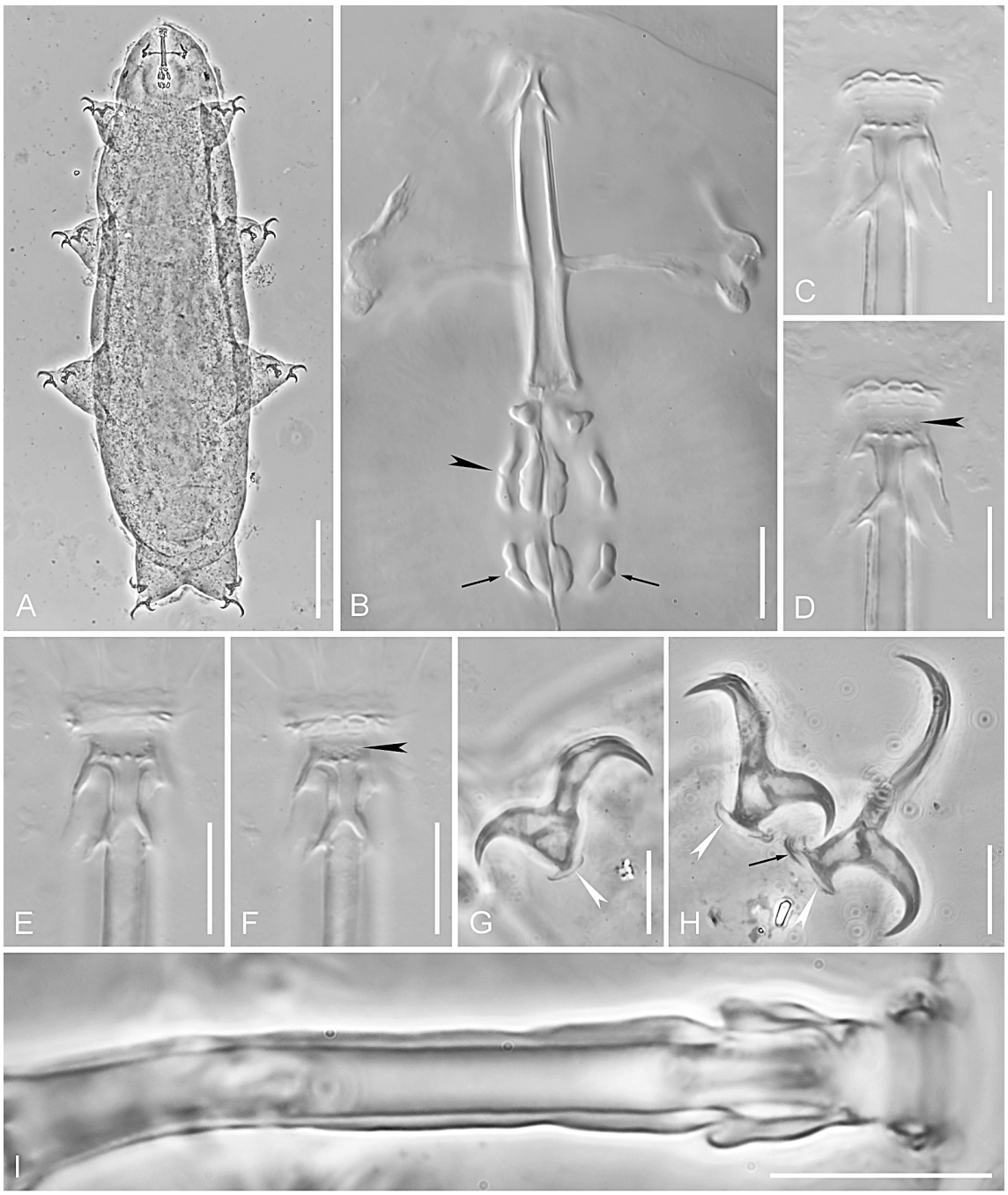

Fig. 3. *Acutuncus antarcticus*. A. Total view, PhC. B. Buccopharyngeal apparatus (black arrowhead indicates constriction of the first macroplacoid, black arrows indicate processes on the second macroplacoids), DIC. C. Dorsal OCA, DIC. D. Dorsal OCA focused on the zone of small teeth (black arrowhead), DIC. E. Ventral OCA, DIC. F. Ventral OCA focused on the zone of small teeth (black arrowhead), DIC. G. Internal claw of the leg II (white arrowheads indicate lunules), PhC. H. Claws IV (white arrowheads indicate lunules, black arrow indicates thickened lunule margin), PhC. I. Buccal tube lateral view, PhC. Scale bars: A = 100 μm, B–I = 10 μm.

surrounded by six indistinct peribuccal lobes (Fig. 4B). In some specimens, a line of elliptical structures visible around mouth opening under LM (Fig. 3C, D, F). Buccopharyngeal apparatus of Hypsibiinae model (Fig. 3B). Oral cavity armature with three bands of teeth. The first band consists of small teeth visible only in the SEM (Fig. 4C, D), and is located on and just behind the ring fold. The second band consists of larger teeth and is faintly visible under LM, in most cases as unclear roughness (Fig. 3D, F; C). The third band consists of largest teeth and is the most posterior and well visible under LM and SEM (Fig. 3C-F; 4C, D). AISMs in form of hooks, asymmetrical with respect to the frontal plane with the dorsal hook being shorter and higher than the ventral with straight or slightly saddle-shaped margin and rounded caudal end (Fig. 3I). Buccal tube rigid and slightly bent ventrally in the caudal part. Stylet furcae typically shaped. Pharyngeal bulb spherical, with well-developed apophyses and two elongate macroplacoids (Fig. 3B). First macroplacoid longer than the second, with distinct constriction in the middle (Fig. 3B; black arrowhead), the anterior end often bears thin, poorly sclerified frontal protrusion, which is poorly visible in young specimens. Second macroplacoid slightly constricted in the middle, usually with a small appendage on external margin (Fig. 3B, black arrows).

All legs with well-developed massive claws, increasing in size from legs I to IV (Fig. 3G, H; Fig. 4E, F). External claws of the *Isohypsibius* type, internal claw of the *Hypsibius* type. All claws with developed accessory points (Fig. 3G, H). Bases of all claws smooth. Claws of all legs with

Table 3
Summary of morphometrics of *Acutuncus antarcticus* from Haswell Island. Primary and secondary branches were measured according to Beasley et al. (2008). Total claw length corresponds to the primary branch length measured according to Pilato et al. (2002).

CHARACTER	N	RANGE						MEAN		SD	
		µm			*pt*			µm	*pt*	µm	*pt*
Body length	30	237	–	570	*859*	–	*1506*	400	*1090*	80	*136*
Buccal tube											
Buccal tube length	30	27.5	–	44.2		–		36.5	–	4.5	–
Stylet support insertion point	30	18.1	–	29.1	*62.1*	–	*66.8*	23.7	*65.1*	2.9	*1.0*
Buccal tube external width	30	2.3	–	4.4	*8.1*	–	*11.0*	3.6	*9.7*	0.7	*0.8*
Buccal tube internal width	30	1.4	–	3.1	*4.6*	–	*8.0*	2.3	*6.3*	0.6	*0.9*
Placoid lengths											
Macroplacoid 1	30	4.9	–	11.4	*15.5*	–	*26.1*	7.8	*21.1*	1.8	*2.8*
Macroplacoid 2	30	3.2	–	6.3	*11.3*	–	*16.4*	4.8	*13.2*	0.9	*1.3*
Macroplacoid row	30	10.1	–	21.0	*32.7*	–	*48.5*	15.0	*40.8*	3.1	*4.2*
Claw 1 lengths											
External base	21	4.5	–	9.6	*14.6*	–	*22.2*	6.7	*18.5*	1.4	*1.9*
External primary branch	21	7.3	–	15.5	*26.6*	–	*39.5*	11.7	*32.1*	2.5	*3.7*
External secondary branch	20	5.4	–	11.9	*19.7*	–	*29.9*	9.2	*25.2*	1.8	*2.4*
External total	21	11.5	–	23.7	*41.6*	–	*56.6*	18.1	*49.5*	3.5	*4.3*
External *cbt* ratio	21	43.3	–	70.5				58.1	–	7.1	–
External *br* ratio	20	67.3	–	90.3				79.5		6.7	
Internal base	25	3.9	–	8.2	*14.1*	–	*19.0*	6.0	*16.4*	1.1	*1.5*
Internal primary branch	24	7.0	–	12.8	*25.2*	–	*33.4*	10.2	*28.2*	1.8	*2.2*
Internal secondary branch	24	5.8	–	12.1	*21.0*	–	*27.9*	8.9	*24.5*	1.6	*2.1*
Internal total	24	8.9	–	16.7	*31.9*	–	*40.4*	13.1	*36.4*	2.2	*2.5*
Internal *cbt* ratio	24	52.4	–	69.5				58.0	–	4.6	–
Internal *br* ratio	23	79.1	–	99.3				87.3		5.9	
Claw 2 lengths											
External base	24	4.7	–	19.2	*15.8*	–	*48.9*	7.8	*21.6*	3.0	*6.4*
External primary branch	24	7.3	–	16.8	*26.4*	–	*41.9*	12.6	*35.0*	2.6	*4.0*
External secondary branch	24	6.5	–	12.4	*22.3*	–	*30.9*	9.6	*26.7*	1.7	*2.2*
External total	24	12.2	–	25.4	*44.1*	–	*63.2*	19.7	*54.7*	3.9	*5.1*
External *cbt* ratio	24	44.7	–	127.6				62.1	–	16.7	–
External *br* ratio	24	58.0	–	99.4				76.9		8.6	
Internal base	25	3.9	–	9.3	*14.2*	–	*21.4*	6.7	*18.1*	1.4	*2.0*
Internal primary branch	24	7.4	–	15.0	*26.6*	–	*35.2*	11.1	*30.5*	1.9	*2.5*
Internal secondary branch	25	6.2	–	12.1	*22.5*	–	*30.3*	9.6	*26.1*	1.6	*2.0*
Internal total	24	9.1	–	19.6	*33.2*	–	*46.0*	14.3	*39.3*	2.7	*3.5*
Internal *cbt* ratio	24	48.7	–	67.9				59.2	–	4.8	–
Internal *br* ratio	24	77.5	–	97.8				86.0		5.0	
Claw 3 lengths											
External base	25	4.8	–	11.0	*16.6*	–	*25.6*	7.8	*21.3*	1.7	*2.5*
External primary branch	25	8.0	–	16.7	*29.0*	–	*43.7*	13.0	*35.5*	2.5	*3.9*
External secondary branch	25	6.3	–	12.4	*22.8*	–	*33.0*	10.1	*27.7*	1.9	*2.5*
External total	24	12.5	–	26.9	*45.5*	–	*66.5*	20.4	*55.9*	3.9	*5.2*
External *cbt* ratio	25	47.6	–	72.4				60.4	–	6.7	–
External *br* ratio	25	66.9	–	92.3				78.5		6.7	
Internal base	27	3.8	–	9.8	*13.8*	–	*22.6*	6.7	*18.2*	1.5	*2.3*
Internal primary branch	27	7.3	–	14.9	*25.6*	–	*34.4*	10.9	*30.0*	1.8	*2.2*
Internal secondary branch	27	6.0	–	11.9	*21.0*	–	*29.9*	9.4	*25.9*	1.7	*2.3*
Internal total	27	9.5	–	20.2	*33.9*	–	*46.6*	14.4	*39.4*	2.8	*3.4*
Internal *cbt* ratio	27	48.4	–	68.9				60.7	–	5.2	–
Internal *br* ratio	27	73.9	–	97.6				86.3		5.5	
Claw 4 lengths											
Anterior base	23	4.6	–	10.6	*16.6*	–	*25.0*	7.6	*20.8*	1.7	*2.3*
Anterior primary branch	23	7.4	–	16.5	*26.7*	–	*37.9*	12.1	*33.1*	2.4	*3.1*
Anterior secondary branch	22	5.3	–	12.1	*19.4*	–	*30.1*	9.5	*26.2*	1.8	*3.0*
Anterior total	23	10.8	–	21.3	*38.7*	–	*49.1*	16.3	*44.9*	3.1	*3.4*
Anterior *cbt* ratio	23	56.2	–	72.8				62.8	–	4.5	–
Anterior *br* ratio	22	58.4	–	89.7				79.5		7.4	
Posterior base	26	5.4	–	11.4	*17.7*	–	*26.1*	8.0	*22.1*	1.4	*2.1*
Posterior primary branch	25	10.3	–	21.4	*36.5*	–	*54.5*	16.7	*46.1*	3.4	*5.4*
Posterior secondary branch	26	6.9	–	14.2	*25.0*	–	*33.4*	10.5	*29.2*	1.7	*2.3*
Posterior total	25	15.7	–	29.9	*56.8*	–	*74.3*	23.9	*66.2*	4.5	*6.0*
Posterior *cbt* ratio	25	40.4	–	58.3				48.2	–	4.9	–
Posterior *br* ratio	25	51.6	–	74.5				63.8		5.9	

smooth lunules (=pseudolunules, according to Gąsiorek et al. 2017) (Fig. 3G, H), better developed on legs IV. Posterior claws on legs IV with thickened region on the lunule margin, visible under LM as a dark line, which can create the impression of the presence of a cuticular bar between the bases of the anterior and posterior claws (Fig. 3H, black arrow).

Eggs. Laid free to the environment (Fig. 5A), 75.7–96.0 µm in diameter (SM.14). Eggshell under LM appears sculptured with granules or short stripes, clearly visible even with low magnification (40x) (Fig. 5C). In fact, these granules are inner pillar-like structures in the eggshell (Fig. 5B, D, F). Under SEM, the outer layer of the eggshell appears as a layer of tightly intertwined fibrous material (Fig. 5F). The outer surface of the eggshell seems to be highly adhesive, as it is usually covered with debris particles.

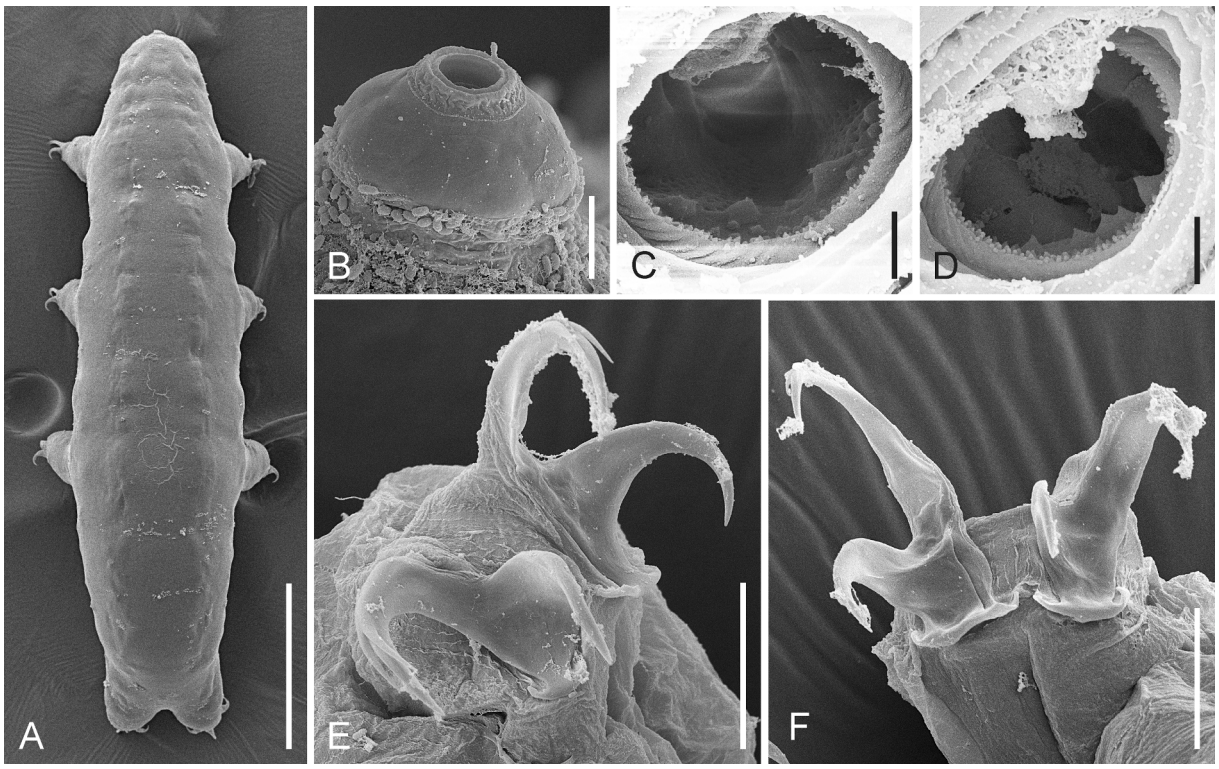

Fig. 4. *Acutuncus antarcticus*. A. Dorsal view. B. Mouth cone. C. Dorsal OCA. D. Ventral OCA. E. Claws III. F. Claws IV. SEM. Scale bars: A = 100 μm, B = 5 μm, C, D = 1 μm, E, F = 10 μm.

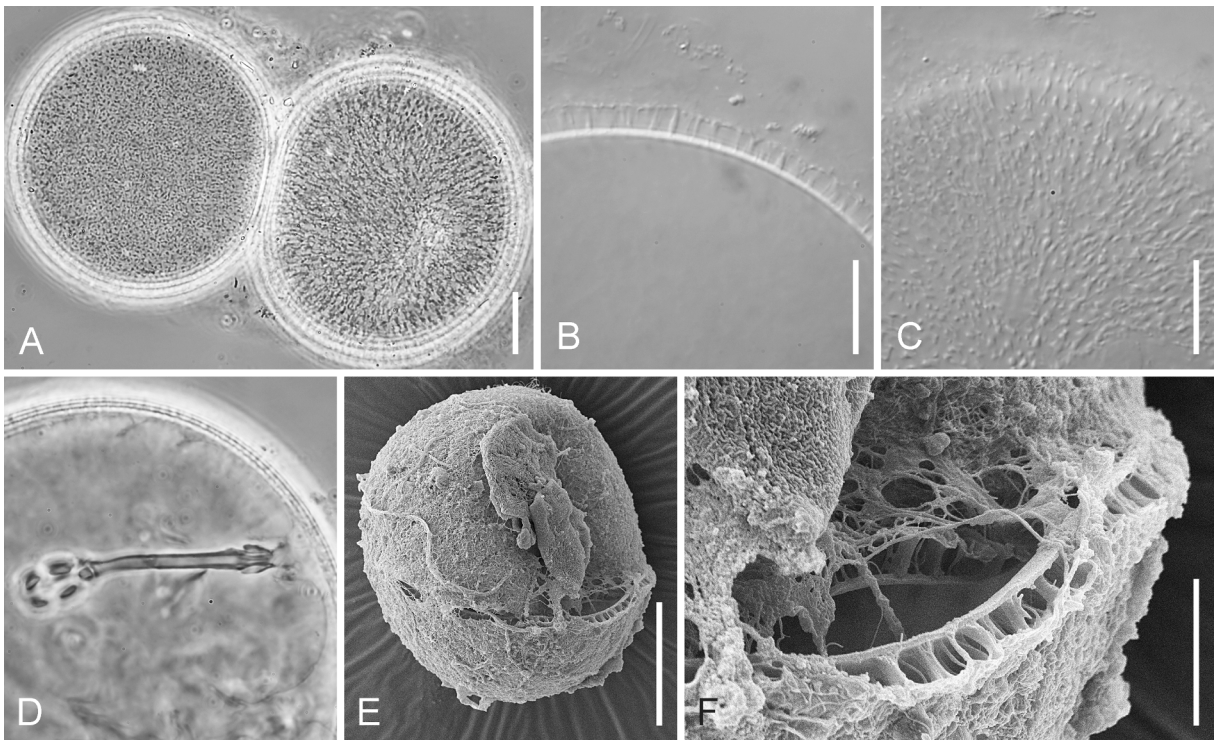

Fig. 5. *Acutuncus antarcticus*. A. Clutch of two eggs demonstrating variability of the eggshell structure, PhC. B. Optical section of the eggshell, DIC. C. Surface view of the eggshell, DIC. D. Optical section of the embryonated egg, PhC. E. Total view of the egg, SEM. F. Damaged eggshell with pillars visible, SEM. Scale bars: A = 20 μm, B-D = 10 μm, E = 20 μm, F = 5 μm.

Reproductive mode. No males were observed, which suggests a parthenogenetic type of reproduction.

DNA sequences. SSU: 3 sequences (OM278639–OM278641); LSU: 3 sequences (OM278642–OM278644); COI: 3 sequences (OM278781–OM278783); ITS2: 3 sequences (OM304858–OM304860).

Species: *Acutuncus mecnuffi* sp. nov.

urn:lsid:zoobank.org:act:A4420739-54D0-42BC-BE5F-32F8B7CEF281

Holotype. Sex indet.; Manchester, UK; gutter moss; 2017; Bob McNuff leg.; Slide S426-SL3-C deposited at St. Petersburg State University.

Paratypes. 105 specimens (and 29 eggs) on slides and 30 specimens on SEM stubs, same data as for holotype (Slides S426-SL1 to SL8, SEM stubs SpbU_29 and S426-stub1). Type specimens are deposited at Department of Biological and Environmental Sciences (Jyväskylä University) (S426_SL8 and S426-stub1) and St Petersburg State University (S426_SL1-7 and stub SpbU_29).

Animals. Body small, elongate, slightly widened at the level of legs III (Fig. 6A–D), with a blunt snout (for comparison see the sharp snout of *Itaquascon*) (morphometrics: Table 4 and Supplementary material SM.15). Body transparent or whitish. No eyespots observed in fixed specimens. Cuticle with rugose sculpture better developed (visible under LM) dorsally, visible over all body surface and on legs under SEM (Fig. 6).

Mouth opening anteroventral, on developed mouth cone (Figs. 6D and 7B); surrounded by six indistinct peribuccal lobes (Fig. 7D). In some specimens, under LM a line of elliptical structures visible around mouth opening (Fig. 7F). Buccopharyngeal apparatus of Hypsibiinae model (Fig. 7A, B). Oral cavity armature with a ring of small teeth located behind the ring fold and a second row of larger teeth (both rows only visible under SEM; Fig. 7E). Under LM, only thin paired transverse crests are visible dorsally and ventrally in the caudal part of the oral cavity (Fig. 7 F, G), ventral crests are connected to an additional short medial crest (Fig. 7G). AISMs in form of hooks, asymmetrical with respect to the frontal plane, with dorsal hook being shorter and higher than the ventral with straight or slightly saddle-shaped margin and round caudal end (Fig. 7B). Buccal tube rigid and slightly bent ventrally in the caudal section (Fig. 7B). Stylet furcae typically shaped. Pharyngeal bulb spherical, with well-developed apophyses and two elongate macroplacoids (Fig. 7A–C). First macroplacoid slightly longer than second, with distinct constriction in the middle (Fig. 7A–C, black arrowheads). Second macroplacoid with poorly visible process on its outer margin (Fig. 7C, white arrowhead).

All legs with well-developed claws, increasing in size from legs I to IV (Fig. 6D, 7H–M). External claws of the *Isohypsibius* type, internal claw of the *Hypsibius* type. All claws with developed accessory points (Fig. 7H, J, L, M). Distal parts of accessory points of exterior claws of legs I–III are often located on the sides of the main claw branch and, in that case, poorly or completely indiscernible with LM (Fig. 7L). Bases of all claws smooth. Claws of all legs with smooth lunules (=pseudolunules, according to Gąsiorek et al. 2017) (Fig. 7H–K) better developed on legs IV. Posterior claws of legs IV with thickened region on the lunule margin, visible under LM as a dark line, which can create the impression of the

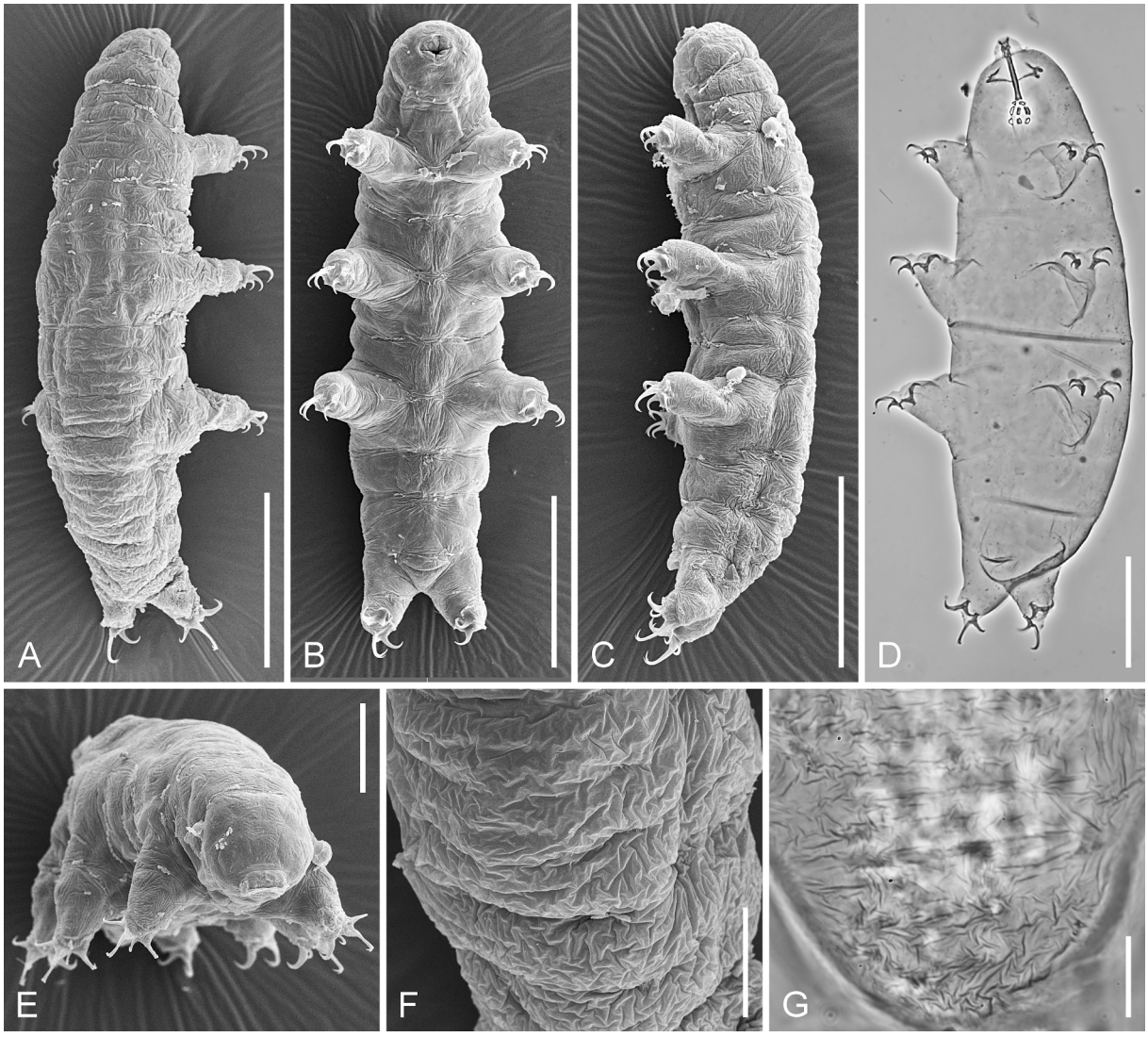

Fig. 6. *Acutuncus mecnuffi* **sp. nov.** A. Dorsal view, SEM. B. Ventral view, SEM. C. Lateral view, SEM. D. Total view, PhC. E. Frontal view, SEM. F. Dorsal sculpture, SEM. G. Dorsal sculpture, PhC. Scale bars: A-D = 50 μm, E = 20 μm, F, G = 10 μm.

Table 4
Summary of morphometrics of *Acutuncus mecnuffi* **sp. nov.** Primary and secondary branches were measured according to Beasley et al. (2008). Total claw length corresponds to the primary branch length measured according to Pilato et al. (2002).

CHARACTER	N	RANGE						MEAN		SD		Holotype	
		µm			*pt*			µm	*pt*	µm	*pt*	µm	*pt*
Body length	29	151	–	256	*727*	–	*1067*	214	*905*	29	*82*	233	*963*
Buccal tube													
Buccal tube length	28	17.2	–	26.1		–		23.7	–	2.3	–	24.2	–
Stylet support insertion point	25	11.7	–	19.5	*58.1*	–	*75.3*	15.3	*64.6*	1.8	*3.9*	16.7	*68.8*
Buccal tube external width	23	1.4	–	2.7	*7.4*	–	*10.9*	2.1	*9.0*	0.3	*0.9*	2.4	*9.9*
Buccal tube internal width	21	0.7	–	1.5	*3.2*	–	*6.1*	1.1	*4.5*	0.2	*0.7*	1.2	*5.1*
Placoid lengths													
Macroplacoid 1	27	2.2	–	4.2	*10.4*	–	*17.9*	3.5	*14.9*	0.5	*1.5*	3.8	*15.6*
Macroplacoid 2	27	2.2	–	3.5	*9.9*	–	*14.1*	2.8	*11.8*	0.4	*1.2*	3.1	*12.6*
Placoid row	27	5.4	–	8.7	*25.0*	–	*40.0*	7.3	*30.7*	0.9	*3.1*	8.5	*35.0*
Claw 1 heights													
External base	16	2.8	–	5.4	*12.1*	–	*20.9*	4.0	*16.7*	0.8	*2.7*	3.8	*15.6*
External primary branch	17	4.6	–	9.4	*27.1*	–	*39.9*	7.8	*33.4*	1.4	*3.6*	7.1	*29.1*
External secondary branch	16	4.0	–	6.7	*19.9*	–	*28.8*	5.6	*23.9*	0.7	*2.4*	5.9	*24.3*
External total	10	8.7	–	12.9	*45.1*	–	*54.3*	11.6	*49.6*	1.6	*2.8*	?	?
External *cbt* ratio	16	34.9	–	67.3		–		52.4	–	9.4	–	53.6	–
External *br* ratio	16	58.0	–	101.3				74.2		11.6			
Internal base	12	2.2	–	4.0	*8.9*	–	*18.3*	3.0	*12.7*	0.7	*3.5*	2.2	*8.9*
Internal primary branch	10	4.6	–	7.3	*25.8*	–	*30.3*	6.4	*27.6*	0.8	*1.4*	6.3	*25.8*
Internal secondary branch	10	3.8	–	6.6	*18.7*	–	*26.7*	5.1	*21.9*	0.8	*2.6*	5.3	*21.8*
Internal total	2	6.6	–	8.2	*34.0*	–	*34.2*	7.4	*34.1*	1.2	*0.2*	?	?
Internal *cbt* ratio	10	34.1	–	59.9		–		45.4	–	10.3	–	34.4	–
Internal *br* ratio	10	66.7	–	93.5				80.4		7.5			
Claw 2 heights													
External base	20	2.5	–	5.8	*10.0*	–	*23.9*	4.4	*18.4*	0.9	*3.4*	4.7	*19.6*
External primary branch	19	5.7	–	10.3	*23.9*	–	*40.8*	8.3	*35.3*	1.4	*4.2*	8.8	*36.2*
External secondary branch	19	3.9	–	7.8	*19.6*	–	*30.3*	6.2	*26.0*	1.2	*3.4*	6.4	*26.5*
External total	12	8.7	–	14.4	*47.3*	–	*58.2*	12.1	*52.7*	1.9	*4.0*	12.3	*50.7*
External *cbt* ratio	19	38.6	–	72.1		–		53.2	–	9.8	–	54.2	–
External *br* ratio	19	56.6	–	89.3				74.6		9.0			
Internal base	17	2.3	–	4.4	*10.2*	–	*19.0*	3.4	*14.8*	0.7	*2.8*	3.0	*12.4*
Internal primary branch	16	5.0	–	8.2	*24.0*	–	*32.6*	6.6	*28.6*	1.0	*2.8*	6.4	*26.2*
Internal secondary branch	17	3.3	–	6.7	*18.7*	–	*26.1*	5.3	*22.5*	0.9	*2.1*	5.0	*20.5*
Internal total	11	6.2	–	9.9	*32.7*	–	*41.6*	8.4	*37.4*	1.4	*2.8*	?	?
Internal *cbt* ratio	16	32.3	–	71.7		–		51.9	–	10.4	–	47.4	–
Internal *br* ratio	16	59.5	–	99.1				78.9		9.8			
Claw 3 heights													
External base	20	2.3	–	6.0	*10.7*	–	*24.1*	4.6	*19.7*	1.1	*3.4*	4.6	*19.0*
External primary branch	20	5.0	–	10.0	*29.0*	–	*42.3*	8.3	*35.5*	1.5	*3.4*	9.4	*38.7*
External secondary branch	20	3.8	–	8.5	*21.2*	–	*32.8*	6.2	*26.6*	1.4	*3.4*	6.2	*25.5*
External total	10	8.6	–	15.2	*46.8*	–	*59.0*	12.4	*52.8*	2.3	*4.4*	13.2	*54.4*
External *cbt* ratio	20	28.3	–	72.6		–		55.7	–	10.3	–	49.2	–
External *br* ratio	20	57.2	–	88.2				75.4		9.9			
Internal base	16	2.1	–	5.0	*8.9*	–	*20.5*	3.8	*15.9*	0.8	*3.0*	5.0	*20.5*
Internal primary branch	12	3.7	–	7.4	*15.5*	–	*29.8*	6.0	*25.2*	1.2	*5.1*	7.0	*28.9*
Internal secondary branch	16	3.3	–	6.8	*14.6*	–	*27.0*	5.2	*21.7*	1.1	*3.4*	4.9	*20.4*
Internal total	7	6.7	–	10.4	*34.3*	–	*40.0*	8.4	*37.3*	1.4	*2.4*	?	*?*
Internal *cbt* ratio	11	33.6	–	97.3		–		61.7	–	15.8	–	71.0	–
Internal *br* ratio	11	70.5	–	145.5				88.5		20.9			
Claw 4 heights													
Anterior base	10	2.8	–	5.6	*12.9*	–	*22.6*	4.0	*17.1*	0.9	*2.8*	4.2	*17.4*
Anterior primary branch	10	4.1	–	8.8	*23.6*	–	*35.3*	7.0	*31.4*	1.6	*3.6*	7.4	*30.5*
Anterior secondary branch	10	2.4	–	8.0	*11.4*	–	*34.2*	5.0	*22.3*	1.5	*6.5*	6.1	*25.3*
Anterior total	10	7.3	–	11.6	*37.9*	–	*46.5*	9.8	*42.0*	1.5	*3.4*	9.6	*39.8*
Anterior *cbt* ratio	9	46.1	–	69.7		–		53.5	–	7.1	–	57.1	–
Anterior *br* ratio	8	48.4	–	102.7				67.4		17.8			
Posterior base	12	2.3	–	5.8	*10.8*	–	*22.4*	4.2	*18.1*	1.2	*3.4*	4.5	*18.5*
Posterior primary branch	13	6.6	–	12.1	*27.4*	–	*50.9*	9.6	*42.0*	1.8	*6.2*	6.6	*27.4*
Posterior secondary branch	12	3.9	–	11.1	*19.2*	–	*46.0*	6.4	*27.6*	2.1	*7.7*	11.1	*46.0*
Posterior total	12	10.9	–	17.2	*52.2*	–	*68.7*	14.6	*61.5*	2.2	*5.2*	15.4	*63.8*
Posterior *cbt* ratio	12	30.2	–	67.5		–		42.7	–	10.6	–	67.5	–
Posterior *br* ratio	12	48.4	–	167.6				69.1		32.4			

presence of a cuticular bar between the bases of the anterior and posterior claws (Fig. 7I, J).

Eggs. 1–2 white subspherical eggs are laid in the exuvium (Fig. 8; N = 25 exuviae with eggs), 61.8–74.7 µm in diameter. Eggshell under LM appears sculptured with minuscule granules, visible only with PhC or DIC under high magnification (Fig. 8C, D). In fact, these granules are inner pillar-like structures within the eggshell (Fig. 8B).

Reproductive mode. No males were observed, which suggests a parthenogenetic type of reproduction.

Phenotypic comparison. Acutuncus mecnuffi **sp. nov.** differs from:

- ***Acutuncus antarcticus*** in having no eyespots, a smaller body length of the adult animals (up to 256 µm in *A. mecnuffi* **sp. nov.** and up to 570 µm in *A. antarcticus*), in having a sculptured cuticle, in having no

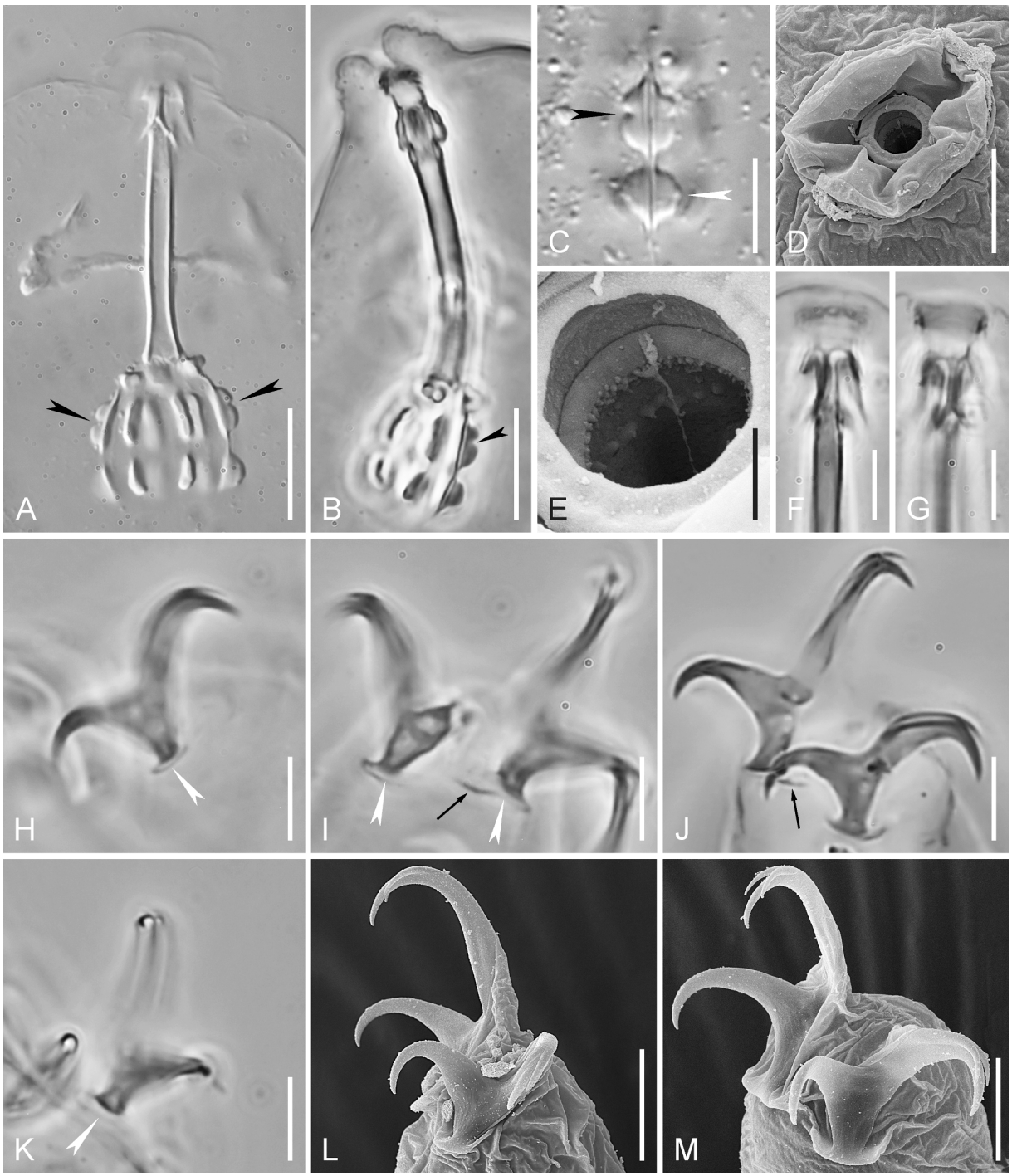

Fig. 7. *Acutuncus mecnuffi* **sp. nov.** A. Buccopharyngeal apparatus, dorso-ventral view (black arrowheads indicate constrictions of the first macroplacoid), DIC. B. Buccopharyngeal apparatus, lateral view (black arrowhead indicates constrictions of the first macroplacoid), PhC. C. Ventral row of macroplacoids (black arrowhead indicates constrictions of the first macroplacoid, white arrowhead indicates process on the second macroplacoid), DIC. D. Mouth opening, SEM. E. Dorsal OCA, SEM. F. Dorsal OCA, PhC. G. Ventral OCA, PhC. H. Internal claw of the leg II (white arrowhead indicates lunule), PhC. I. Claws IV (white arrowheads indicate lunules, black arrow indicates thickened lunule margin), PhC. J. Claws IV (black arrow indicates thickened lunule margin), PhC. K. External claw of the leg III (white arrowhead indicates lunule), PhC. L. Claws III, SEM. M. Claws IV, SEM. Scale bars: A, B = 10 μm, C, D, F–M = 5 μm, E = 1 μm.

rows of large (clearly discernible under LM) teeth in OCA, and in having an eggshell with short internal pillars visible with PhC or DIC only under high magnification (long pillars quite discernible under LM even at low magnification are typical for *A. antarcticus*).

- ***Acutuncus giovanniniae* sp. nov.** in having internal (anterior on legs IV) claws without widened primary branches at the point at which the accessory points diverge from the main branch and in having both dorsal and ventral paired transverse crests in OCA in form of thin arcuate lines (*A. giovanniniae* **sp. nov.** have ventral crests more developed and straighter than dorsal).
- ***Acutuncus mariae*** in having a sculptured cuticle and in having relatively shorter claws (*pt* value for anterior/posterior legs IV primary claw branches is 23.6–35.3/27.4–50.9 in *A. mecnuffi* **sp. nov.** and 39.5–56.2/ 52.0–72.3 in *A. mariae*).

DNA sequences. SSU: 2 sequences (OM350032 and OM350033); LSU:

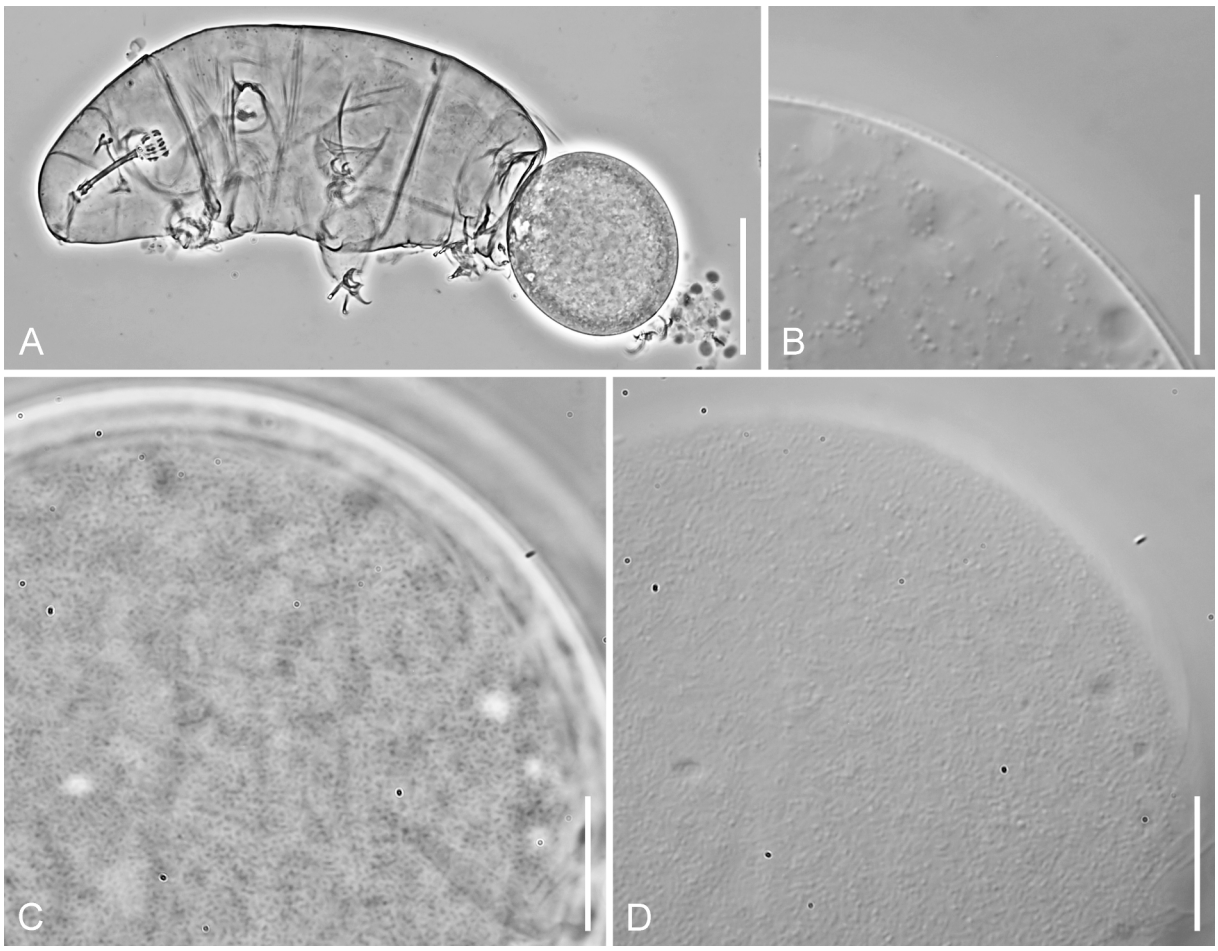

Fig. 8. *Acutuncus mecnuffi* **sp. nov.** A. Egg laying female, PhC. B. Optical section of the eggshell, DIC. C. Surface view of the eggshell, PhC. D. Surface view of the eggshell, DIC. Scale bars: A = 50 μm, B–D = 10 μm.

2 sequences (OM350028 and OM350029); COI: 1 sequence (OM350039).

Etymology. This species is dedicated to Robert McNuff to acknowledge his contribution to tardigrade studies by isolating and sharing the laboratory line of *Hypsibius exemplaris*, now widely used as model organism, and for providing the individuals used for the description of this species.

Species: *Acutuncus giovanniniae* sp. nov.

Urn:lsid:zoobank.org:act:68D6E467-5102-403E-A539-9EC92C62786F.

Mixibius sp. in Vecchi et al. (2022).

Holotype. Sex indet.; Parma, Italy, (44.387421, 10.020868, 1651 m a.s.L.); ephemeral freshwater rock pool sediment; 24 June 2020; Matteo Vecchi and Claudio Ferrari leg.; Slide S283-SL1-3 deposited at St. Petersburg State University.

Paratypes. 50 specimens (and 37 eggs) on slides and 17 specimens on SEM stubs, same data as for holotype (Slides S283-SL1 to SL5, SEM stubs SpbU_31 and S283-stub1). Type specimens are deposited at Department of Biological and Environmental Sciences (Jyväskylä University) (S283_SL5 and S283-stub1) and St. Petersburg State University (S283_SL1-4 and stub SpbU_31).

Animals. Body small, elongate, slightly widened at the level of legs III (Fig. 9A, D), with a blunt snout (for comparison see the sharp snout of *Itaquascon*) (morphometrics: Table 5 and Supplementary material SM.16). Body transparent or whitish. No eyespots observed in live specimens. Under LM, cuticle with rugose sculpture well developed dorsally, usually in caudal region only (Fig. 9F); under SEM sculpture is visible over all body surface and on legs (Fig. 9A–C, E, F).

Mouth opening anteroventral, on developed mouth cone (Fig. 10D). In some specimens, under LM a line of elliptical structures visible around mouth opening (Fig. 10E). Buccopharyngeal apparatus of Hypsibiinae model (Fig. 10A, B). Under LM, only thin paired transverse crests are visible dorsally and ventrally in the caudal part of the oral cavity (Fig. 10E, F), dorsal crests are distinctly arcuate and sometimes with poorly visible granules on their anterior margin (teeth?), ventral crests are more developed and straighter than dorsal (Fig. 10F). AISMs in form of hooks, asymmetrical with respect to the frontal plane and with the dorsal hook being shorter and higher than the ventral with straight or slightly saddle-shaped margin and round caudal end (Fig. 10B). Buccal tube rigid and slightly bent ventrally in caudal part (Fig. 10B). Stylet furcae typically shaped. Pharyngeal bulb spherical, with well-developed apophyses and two elongate macroplacoids (Fig. 10A–C). First macroplacoid slightly longer than second, with distinct constriction in the middle (Fig. 10A–C, black arrowheads). Second macroplacoid with poorly visible process on its outer margin (Fig. 10C, white arrowhead).

All legs with well-developed claws, increasing in size from legs I to IV (Fig. 9D, 10G–J). External claws of the *Isohypsibius* type, internal claw of the *Hypsibius* type. All claws with developed accessory points (Fig. 10H–J). Primary branches of internal (anterior on legs IV) claws obviously widened at the point at which the accessory points diverge from the main branch. (Fig. 10I). Bases of all claws smooth. Claws of all legs with smooth lunules (=pseudolunules, according to Gąsiorek et al. 2017) (Fig. 10G, H, white arrowheads) better developed on legs IV. Posterior claws of legs IV (and rarely external claws of legs I–III) with thickened region on the lunule margin, visible under LM as a dark line, which can create the impression of the presence of a cuticular bar

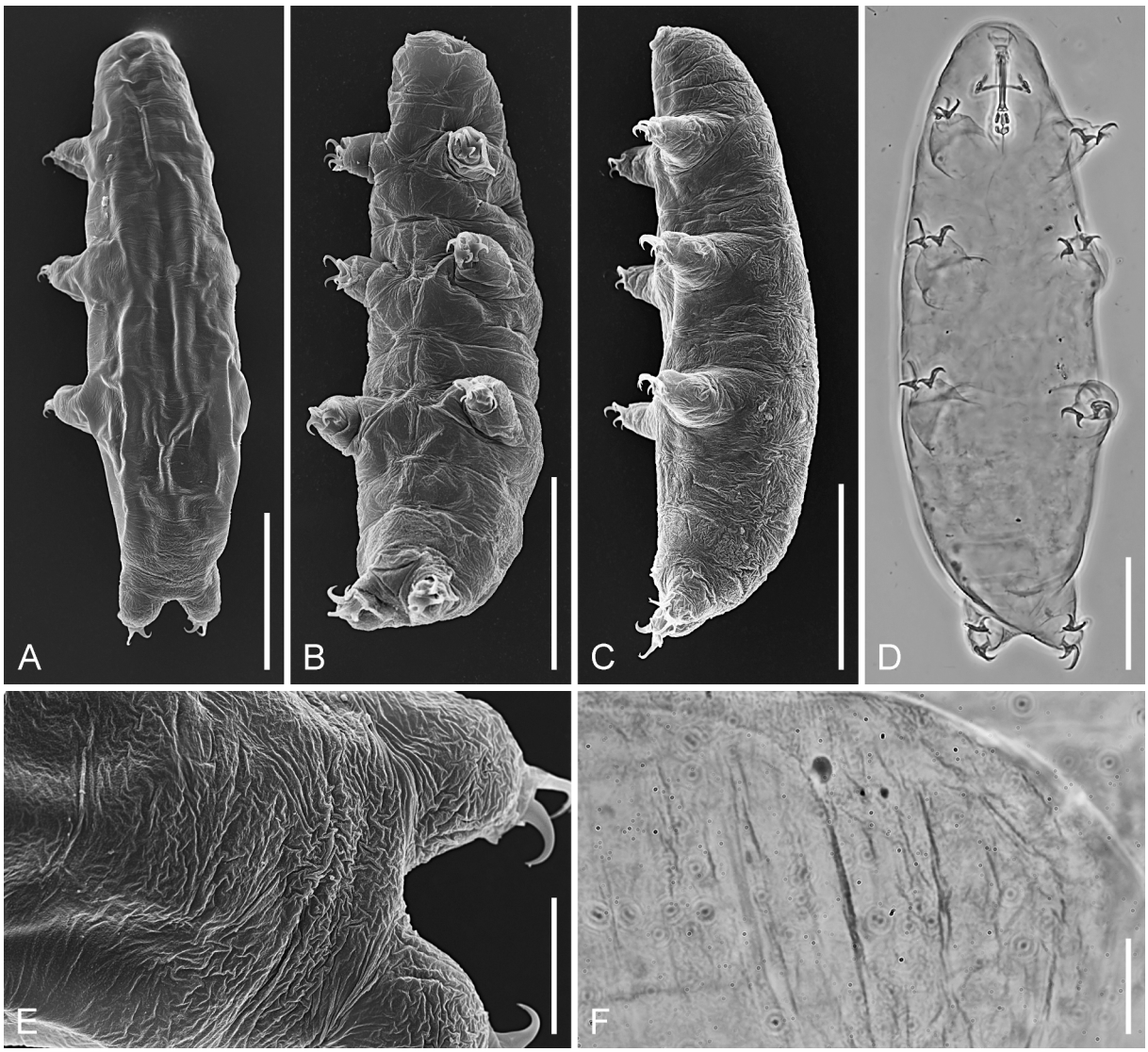

Fig. 9. *Acutuncus giovanniniae* **sp. nov.** A. Dorsal view, SEM. B. Ventral view, SEM. C. Lateral view, SEM. D. Total view, PhC. E. Sculpture of the caudal body region, SEM. F. Sculpture of the caudal body region, PhC. Scale bars: A–D = 50 μm, E, F = 10 μm.

between the bases of the anterior and posterior claws (Fig. 10G, H, black arrows).

Eggs. 1 to 6 (usually 1–2) white subspherical eggs are laid in the exuvium (Fig. 11), 58.3–64.0 μm in diameter. Under LM, eggshell appears sculptured with minuscule granules, visible only with PhC or DIC at high magnification (Fig. 11C, D). In fact, these granules are inner pillar-like structures within the eggshell (Fig. 11B).

Reproductive mode. No males were observed, which suggests a parthenogenetic type of reproduction.

Phenotypic comparison. Acutuncus giovanniniae **sp. nov.** differs from:

- ***Acutuncus antarcticus*** in having no eyespots, a smaller body length of adult animals (up to 271 μm in *A. giovanniniae* **sp. nov.** and up to 570 μm in *A. antarcticus*), in having a sculptured cuticle, in having no rows of large (clearly discernible under LM) teeth in OCA, and in having an eggshell with short internal pillars visible with PhC or DIC only under high magnification (long pillars quite discernible under LM even at low magnification are typical for *A. antarcticus*).
- ***Acutuncus mariae*** in having a sculptured cuticle and in having relatively shorter claws (*pt* value for anterior/posterior legs IV primary claw branches is 22.5–28.2/30.8–38.8 in *A. giovanniniae* **sp. nov.** and 39.5–56.2/52.0–72.3 in *A. mariae*).
- ***Acutuncus mecnuffi*** sp. nov. in having internal (anterior on legs IV) claws with widened primary branches at the point at which the accessory points diverge from the main branch and in having ventral crests in OCA more developed and straighter than dorsal (*A. mecnuffi* **sp. nov.** have both dorsal and ventral paired transverse crests in form of thin arcuate lines).

DNA sequences. SSU: 2 sequences (OM350034 and OM350035); LSU: 2 sequences (OM350030 and OM350031); COI: 6 sequences (MW306851–MW306856); ITS2: 1 sequence (OM401658).

Etymology. We dedicate the species to Ilaria Giovannini, a tardigradologist with research interest focused on the response and adaptations of tardigrades (in particular of *Acutuncus antarcticus*) to global warming.

Eggshell morphology and species morhogroups

All *Acutuncus* species have the same type of chorion. In this case, the eggshell consists of a thick inner layer and a very thin membranous outer layer, with elongated radial pillars forming a layer between (Dastych, 1991, Zawierucha et al. 2020; Figs. 5, 8, 11). Under SEM, the outer layer (reported only for *A. antarcticus*) is composed of densely organised fibrous material (Kagoshima et al. 2013; Cesari et. al., 2016a; Fig. 5E, F). Within this type of eggshell organisation, two clearly different subtypes

Table 5
Summary of morphometrics of *Acutuncus giovanniniae* **sp. nov.** Primary and secondary branches were measured according to Beasley et al. (2008). Total claw length corresponds to the primary branch length measured according to Pilato et al. (2002).

CHARACTER	N	RANGE						MEAN		SD		Holotype	
		µm			*pt*			µm	*pt*	µm	*pt*	µm	*pt*
Body length	17	186	–	271	*758*	–	*1065*	217	*867*	24	*80*	253	*950*
Buccal tube													
Buccal tube length	20	23.1	–	26.6		–		25.1	–	0.9	–	26.6	–
Stylet support insertion point	20	15.1	–	17.5	*62.9*	–	*68.8*	16.5	*65.6*	0.6	*1.2*	17.5	*65.6*
Buccal tube external width	20	2.2	–	2.7	*8.8*	–	*10.4*	2.4	*9.5*	0.2	*0.5*	2.6	*9.7*
Buccal tube internal width	20	1.3	–	1.7	*5.2*	–	*6.7*	1.5	*5.9*	0.1	*0.3*	1.5	*5.6*
Placoid lengths													
Macroplacoid 1	20	3.2	–	4.7	*12.9*	–	*18.5*	3.7	*14.7*	0.4	*1.4*	4.1	*15.5*
Macroplacoid 2	20	2.4	–	3.4	*9.7*	–	*13.3*	2.9	*11.3*	0.3	*1.2*	3.4	*12.6*
Macroplacoid row	20	7.1	–	8.9	*28.1*	–	*34.9*	7.8	*30.8*	0.6	*1.7*	8.5	*32.0*
Claw 1 lengths													
External base	9	3.7	–	4.7	*14.3*	–	*19.5*	4.0	*16.1*	0.3	*1.5*	?	*?*
External primary branch	7	6.0	–	8.6	*23.8*	–	*34.4*	6.8	*27.6*	0.9	*3.7*	?	*?*
External secondary branch	8	4.7	–	6.0	*19.0*	–	*24.7*	5.2	*20.8*	0.4	*1.8*	?	*?*
External total	7	8.4	–	10.8	*34.0*	–	*43.1*	9.6	*38.4*	0.9	*3.1*	?	*?*
External *cbt* ratio	7	43.1	–	66.4		–		58.4	–	7.5	–	?	–
External *br* ratio	6	70.8	–	83.9				78.9		5.6			
Internal base	12	3.1	–	4.3	*12.1*	–	*16.7*	3.4	*13.5*	0.3	*1.2*	3.8	*14.2*
Internal primary branch	12	5.0	–	7.4	*19.6*	–	*29.1*	5.6	*22.3*	0.7	*2.6*	6.1	*22.8*
Internal secondary branch	11	4.2	–	6.4	*18.3*	–	*25.1*	4.9	*19.6*	0.7	*2.2*	6.0	*22.7*
Internal total	12	6.5	–	9.0	*26.6*	–	*35.2*	7.5	*29.9*	0.7	*2.3*	8.3	*31.2*
Internal *cbt* ratio	12	54.3	–	67.5		–		60.7	–	3.8	–	62.1	–
Internal *br* ratio	11	78.9	–	99.5				89.0		6.1			
Claw 2 lengths													
External base	14	3.4	–	5.4	*13.5*	–	*21.1*	4.4	*17.4*	0.6	*2.2*	5.2	*19.4*
External primary branch	13	6.2	–	9.0	*24.4*	–	*36.7*	7.5	*30.0*	1.0	*3.7*	8.6	*32.4*
External secondary branch	14	4.8	–	6.7	*19.1*	–	*26.5*	5.5	*22.0*	0.6	*2.5*	6.7	*25.0*
External total	12	9.3	–	14.1	*37.0*	–	*55.2*	11.2	*44.3*	1.3	*5.0*	12.1	*45.5*
External *cbt* ratio	13	44.1	–	75.3		–		58.0	–	7.3	–	60.0	–
External *br* ratio	13	64.4	–	81.4				73.3		5.7			
Internal base	10	3.1	–	4.6	*12.7*	–	*17.9*	3.6	*14.3*	0.4	*1.5*	3.8	*14.4*
Internal primary branch	10	5.5	–	7.6	*22.8*	–	*30.0*	6.3	*24.9*	0.6	*2.2*	6.7	*25.0*
Internal secondary branch	10	4.4	–	6.6	*17.5*	–	*25.9*	5.2	*20.7*	0.6	*2.2*	5.8	*21.7*
Internal total	10	7.2	–	10.6	*30.1*	–	*41.7*	8.4	*33.0*	1.0	*3.5*	8.9	*33.5*
Internal *cbt* ratio	10	48.2	–	63.0		–		57.5	–	4.3	–	57.7	–
Internal *br* ratio	10	72.9	–	90.6				83.2		5.9			
Claw 3 lengths													
External base	12	3.9	–	5.4	*15.5*	–	*20.4*	4.7	*18.6*	0.4	*1.4*	5.4	*20.4*
External primary branch	10	6.6	–	9.1	*26.1*	–	*35.4*	7.8	*30.8*	1.0	*3.4*	9.1	*34.1*
External secondary branch	12	4.9	–	6.5	*19.3*	–	*24.5*	5.7	*22.8*	0.4	*1.4*	6.5	*24.5*
External total	10	10.1	–	13.7	*42.3*	–	*53.6*	11.8	*46.6*	1.0	*3.4*	12.9	*48.3*
External *cbt* ratio	10	51.6	–	73.3		–		61.4	–	7.3	–	59.8	–
External *br* ratio	10	66.9	–	88.7				75.3		7.9			
Internal base	14	3.2	–	4.6	*12.6*	–	*18.0*	3.6	*14.1*	0.4	*1.3*	3.8	*14.4*
Internal primary branch	14	5.4	–	7.9	*21.4*	–	*31.1*	6.2	*24.4*	0.7	*2.5*	6.8	*25.7*
Internal secondary branch	14	4.4	–	6.3	*18.8*	–	*24.7*	5.2	*20.7*	0.6	*1.8*	6.2	*23.3*
Internal total	14	7.3	–	10.9	*28.5*	–	*42.8*	8.2	*32.3*	0.9	*3.4*	8.7	*32.7*
Internal *cbt* ratio	14	53.3	–	62.3		–		58.1	–	2.7	–	56.1	–
Internal *br* ratio	14	78.7	–	93.9				85.2		5.3			
Claw 4 lengths													
Anterior base	11	3.5	–	4.3	*14.4*	–	*17.2*	3.9	*15.5*	0.3	*0.9*	4.2	*15.9*
Anterior primary branch	11	5.9	–	6.9	*22.5*	–	*28.2*	6.3	*24.9*	0.3	*1.8*	6.0	*22.5*
Anterior secondary branch	11	4.7	–	5.7	*17.8*	–	*22.2*	5.1	*20.3*	0.4	*1.6*	4.7	*17.8*
Anterior total	11	8.1	–	9.9	*31.9*	–	*38.6*	9.0	*35.8*	0.6	*2.5*	9.4	*35.4*
Anterior *cbt* ratio	11	56.6	–	71.7		–		62.3	–	5.0	–	70.7	–
Anterior *br* ratio	11	76.3	–	96.1				81.6		6.5			
Posterior base	10	3.4	–	5.0	*14.5*	–	*20.8*	4.2	*16.9*	0.5	*1.8*	4.7	*17.5*
Posterior primary branch	10	7.8	–	10.1	*30.8*	–	*38.8*	8.7	*35.0*	0.8	*2.7*	10.1	*37.9*
Posterior secondary branch	10	4.2	–	6.6	*18.3*	–	*24.7*	5.4	*21.7*	0.7	*2.0*	6.6	*24.7*
Posterior total	10	11.5	–	14.5	*47.0*	–	*56.2*	12.8	*51.4*	0.9	*3.0*	14.5	*54.5*
Posterior *cbt* ratio	10	41.8	–	58.7		–		48.3	–	5.6	–	46.2	–
Posterior *br* ratio	10	52.7	–	71.8				62.3		6.4			

can be found: one with shorter (below 1.1 µm) and the other with longer (1.7–3.0 µm) pillars within the shell. Eggs of the first morphotype are laid within the exuvium, while eggs of the second morphotype are usually laid free, though singular cases of the second morphotype laying eggs within the exuvium are known (Utsugi and Ohyama, 1989; McInnes, 1995; Kagoshima et a., 2013; Tumanov, 2020a). Currently, the distribution of the eggshell morphotypes coincides with the geographical distribution of *Acutuncus* species as well as with the reconstructed phylogeny of the genus. Eggs of the first morphotype are typical for the monophyletic European clade comprising *A. mariae*, *A. mecnuffi* **sp. nov.**, and *A. giovanniniae* **sp. nov.**, whereas the second morphotype is typical for the Antarctic group of species, which appears as paraphyletic in the reconstructed phylogeny (Fig. 2). This type of the eggshell structure is not a unique character for the *Acutuncus* clade. The

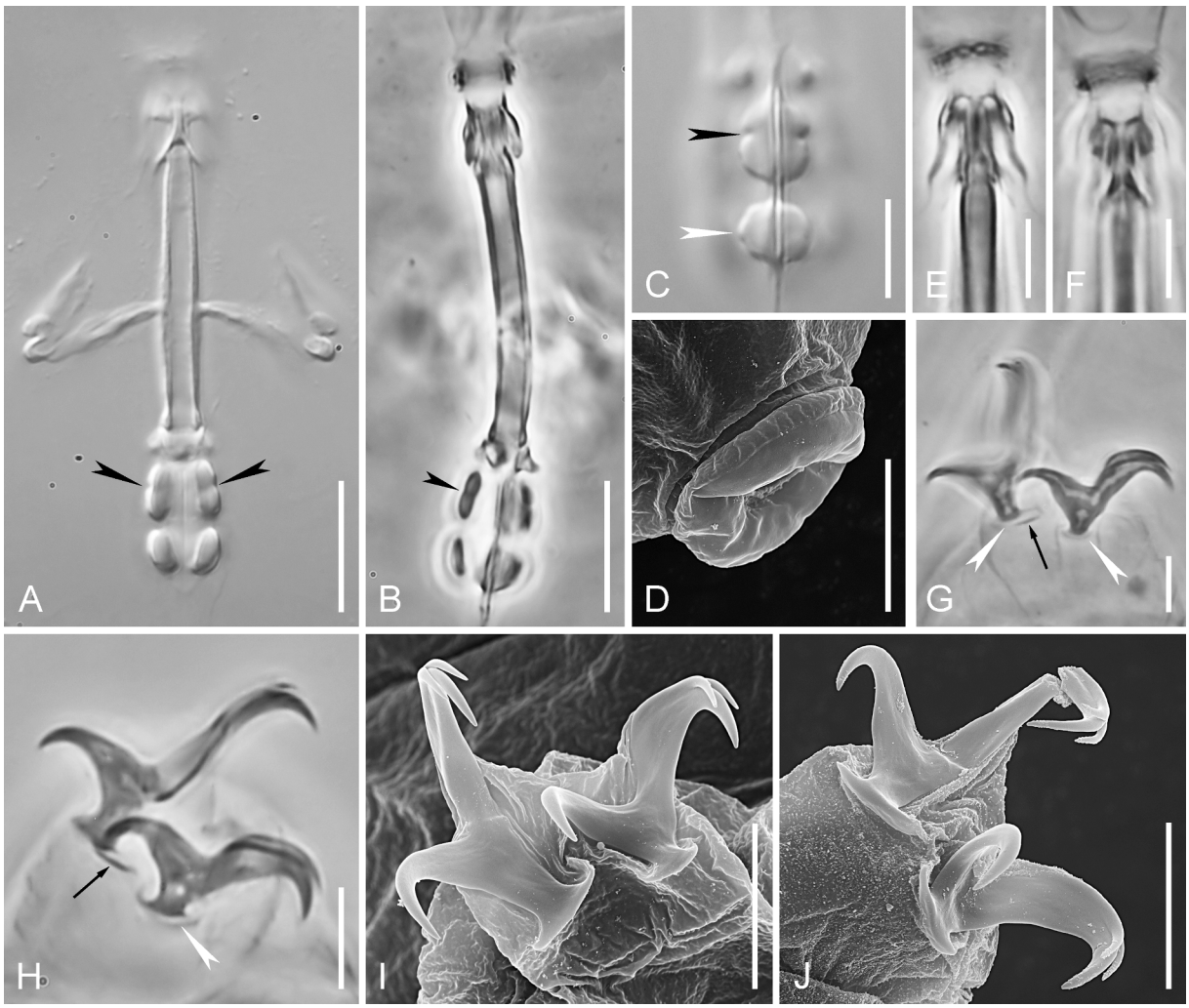

Fig. 10. *Acutuncus giovanniniae* **sp. nov.** A. Buccopharyngeal apparatus, dorso-ventral view (black arrowheads indicate constrictions of the first macroplacoid), DIC. B. Buccopharyngeal apparatus, lateral view (black arrowhead indicates constrictions of the first macroplacoid), PhC. C. Ventral row of macroplacoids (black arrowhead indicates constriction of the first macroplacoid, white arrowhead indicates process on the second macroplacoid), DIC. D. Mouth cone, SEM. E. Dorsal OCA, PhC. F. Ventral OCA, PhC. G. Claws II (white arrowheads indicate lunules, black arrow indicates thickened lunule margin), PhC. H. Claws IV (white arrowhead indicates lunule, black arrow indicates thickened lunule margin), PhC. I. Claws II, SEM. J. Claws IV, SEM. Scale bars: A, B = 10 μm, C-J = 5 μm.

same type of eggshell is known for different groups within Hypsibiidae: the genera *Notahypsibius* and *Pilatobius* (Pilatobiinae; Tumanov, 2020a), and two species of the genus *Hypsibius* (*H. roanensis* Nelson and McGlothlin, 1993 and *H.* cf. *scabropygus*; Hypsibiinae; (Guidetti et al. 1999; Guidetti and Bertolani, 2001). Due to the presence of two different eggs morphotypes in the genus *Acutuncus* and the non-monophyly of both groups of species producing them, we propose two morpho-groups of species (*sensu* Stec et al., 2021, i.e.: a non-monophyletic group of morphologically similar species):

- ***Acutuncus antarcticus* morphogroup**: Eggs laid free (or occasionally in exuvium) with long pillars (1.7–3.0 μm) usually forming a striated pattern on the egg surface. Composition: *Acutuncus antarcticus* (Richters, 1904), *Acutuncus* sp. [Ca. 1 Vecchi et al., 2023].
- ***Acutuncus mariae* morphogroup**: Eggs laid in exuvium, with short pillars (<1.1 μm) usually forming a dotted pattern of the egg surface. Composition: *Acutuncus mariae* Zawierucha, 2020, *Acutuncus mecnuffi* **sp. nov.** Vecchi, Tsvetkova, Stec, Ferrari, Calhim, Tumanov, 2023, *Acutuncus giovanniniae* **sp. nov.** Vecchi, Tsvetkova, Stec, Ferrari, Calhim, Tumanov, 2023.

6. Conclusions

The collection and phylogenetic analysis of two new populations of *Acutuncus* from Europe (UK and Italy) greatly extends the known range (geographical and environmental) of this genus, once thought to be exclusively polar (Antarctica and Svalbard). The new data allows us to divide the genus into two phenotypically distributable species groups and to institute a new monotypic family Acutuncidae **fam. nov.** which accommodates all members of the genus *Acutuncus*.

CRediT authorship contribution statement

M. Vecchi: Conceptualization, Formal analysis, Investigation, Data curation, Writing – original draft, Visualization, Supervision, Project administration. **AY. Tsvetkova:** Investigation, Writing – review & editing. **D. Stec:** Investigation, Writing – review & editing, Resources. **C. Ferrari:** Investigation, Writing – review & editing. **S. Calhim:** Resources, Funding acquisition, Writing – review & editing. **D.V. Tumanov:** Conceptualization, Formal analysis, Investigation, Data curation, Writing – original draft, Visualization, Supervision, Project administration, Resources, Funding acquisition.

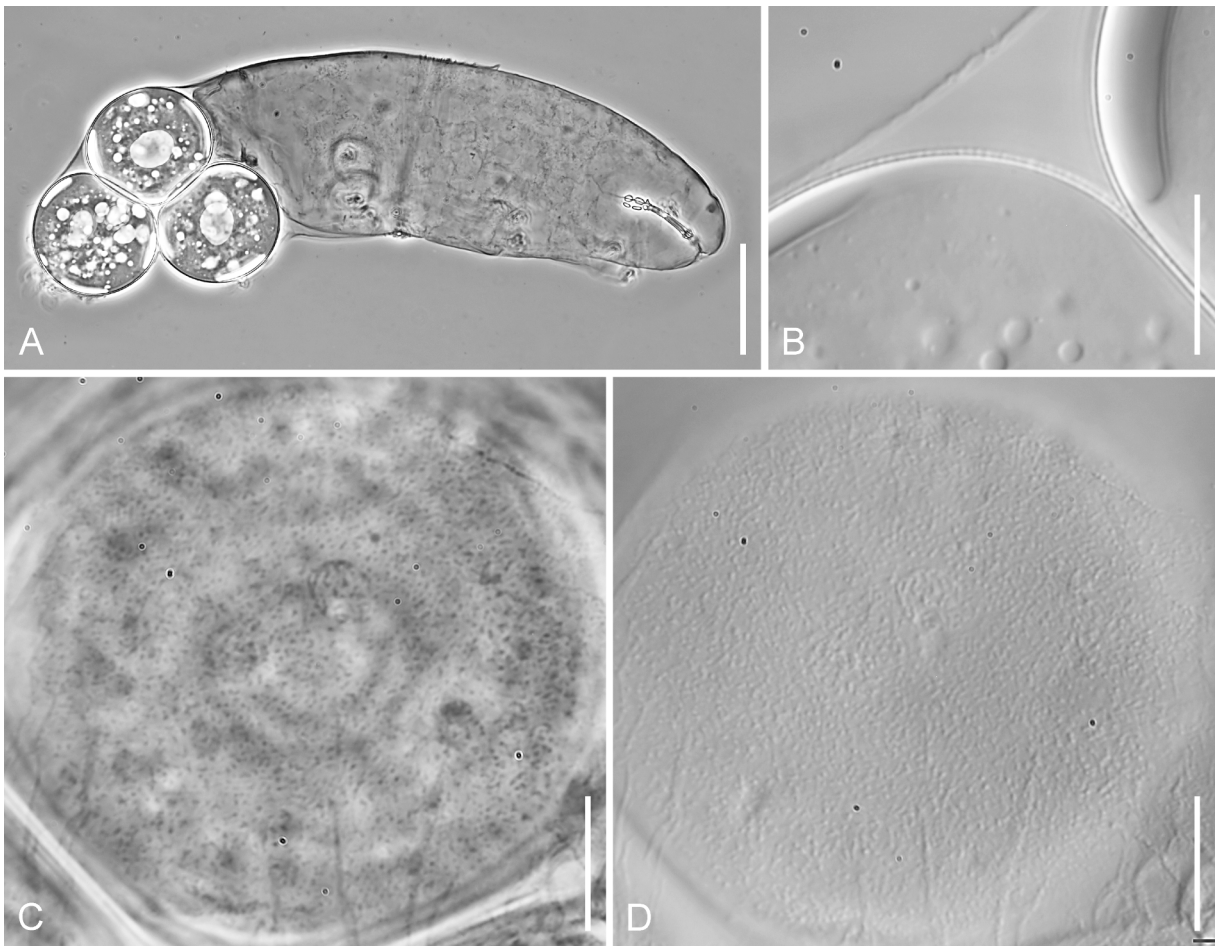

Fig. 11. *Acutuncus giovanniniae* **sp. nov.** A. Egg laying female, PhC. B. Optical section of the eggshell, DIC. C. Surface view of the eggshell, PhC. D. Surface view of the eggshell, DIC. Scale bars: A = 50 μm, B-D = 10 μm.

Declaration of Competing Interest

The authors declare that they have no known competing financial interests or personal relationships that could have appeared to influence the work reported in this paper.

Data availability

All the data produced in this study is made available in GenBank (DNA sequences) or as Supplementary Material to this article (morphometric data).

Acknowledgements

We wish to acknowledge Bob McNuff (Sciento, UK) for providing *A. mecnuffi* individuals. Sample S283 (with *A. giovanniniae*) was collected under sampling permit Prot.1972/2020 issued to M.V. by Parco Nazionale Appennino Tosco-Emiliano (Massa-Carrara, Italy). We are grateful to Dr Boris Anokhin (Zoological Institute, Russia) for providing fixed material of *A. antarcticus,* collected during the 29th Russian Antarctic expedition. We are also grateful to Dr. Alexei Smirnov and Galina Avdeeva (SPbU, Russia) for collecting material in the Murmansk region, and in the St. Petersburg region. We would like to thank the reviewers for valuable comments and suggestions, which helped us to improve the manuscript. This study was carried out with the use of equipment of the Core Facilities Center "Centre for Molecular and Cell Technologies" of St. Petersburg State University and of the Nanoscience Center of University of Jyväskylä. The study was supported by an Academy of Finland Fellowships to S.C. (#314219 and #335759). The work of D. Tumanov was supported by the State scientific program "Taxonomy, biodiversity and ecology of invertebrates from Russian and adjacent waters of World Ocean, continental water bodies and damped areas" No. 1021051402797-9. This work and the new species name were registered with ZooBank under urn:lsid:zoobank.org:pub:D72B9B17-EDBB-4F4D-8ADC-78B4ADD00566.

Appendix A. Supplementary material

Supplementary data to this article can be found online at https://doi.org/10.1016/j.ympev.2023.107707.

References

Aberer, A.J., Krompass, D., Stamatakis, A., 2013. Pruning rogue taxa improves phylogenetic accuracy: an efficient algorithm and webservice. Syst. Biol. 62 (1), 162–166. https://doi.org/10.1093/sysbio/sys078.

Bah, T., 2011. Inkscape: Guide to A Vector Drawing Program, vol. 559. Prentice Hall, Upper Saddle River, NJ, USA.

Beasley, C.W., Kaczmarek, Ł., Michalczyk, Ł., 2008. *Doryphoribius mexicanus*, a new species of Tardigrada (Eutardigrada: hypsibiidae) from Mexico (North America). Proc. Biol. Soc. Wash. 121 (1), 34–40. https://doi.org/10.2988/07-30.1.

Bertolani, R., Guidetti, R., Marchioro, T., Altiero, T., Rebecchi, L., Cesari, M., 2014. Phylogeny of Eutardigrada: New molecular data and their morphological support lead to the identification of new evolutionary lineages. Mol. Phylogenet. Evol. 76, 110–126.

Betancur-R., R., Naylor, G. J. P., Ortí, G., 2014. Conserved genes, sampling error, and phylogenomic inference. System. Biol. 63, 257–262. <https://doi.org/10.1093/sysbi o/syt073>.

Cesari, M., McInnes, S.J., Bertolani, R., Rebecchi, L., Guidetti, R., 2016a. Genetic diversity and biogeography of the south polar water bear *Acutuncus antarcticus*

(Eutardigrada : Hypsibiidae) – evidence that it is a truly pan-Antarctic species. Invertebr. Syst. 30, 635–649. https://doi.org/10.1071/IS15045.
Cesari, M., Vecchi, M., Palmer, A., Bertolani, R., Pilato, G., Rebecchi, L., Guidetti, R., 2016b. What if the claws are reduced? Morphological and molecular phylogenetic relationships of the genus *Haplomacrobiotus* May, 1948 (Eutardigrada, Parachela). Zool. J. Linn. Soc 178, 819–827. https://doi.org/10.1111/zoj.12424.
Chen, M.-Y., Liang, D., Zhang, P., 2015. Selecting question-specific genes to reduce incongruence in phylogenomics: a case study of jawed vertebrate backbone phylogeny. System. Biol. 64, 1104–1120. https://doi.org/10.1093/sysbi o/syv059.
Czechowski, P., Sands, C.J., Adams, B.J., D'Haese, C.A., Gibson, J.A.E., McInnes, S.J., Stevens, M.I., 2012. Antarctic Tardigrada: a first step in understanding molecular operational taxonomic units (MOTUs) and biogeography of cryptic meiofauna. Invertebr. Syst. 26, 526–538. https://doi.org/10.1071/IS12034.
Dastych, H., 1991. Redescription of *Hypsibius antarcticus* (Richters, 1904), with some notes on Hypsibius arcticus (Murray, 1907) (Tardigrada). Mitteilungen aus dem hamburgischen zoologischen Museum und Institut 88, 141–159.
Degma, P., Guidetti, R., 2022. Actual checklist of Tardigrada species. Università di Modena e Reggio Emilia. <https://dx.doi.org/10.25431/11380_1178608>.
Degma, P., Guidetti, R., 2007. Notes to the current checklist of Tardigrada. Zootaxa. 1579 (1), 41–53. https://doi.org/10.11646/zootaxa.1579.1.2.
Doyère, M.L., 1840. Memorie sur les Tardigrades. Ann. Sci. Naturel. Zool. 14, 269–362.
Edgar, R., 2004. MUSCLE: multiple sequence alignment with high accuracy and high throughput. Nucl. Acids Res. 32 (5), 1792–1797. https://doi.org/10.1093/nar/gkh340.
Gąsiorek, P., Zawierucha, K., Stec, D., Michalczyk, Ł., 2017. Integrative redescription of a common Arctic water bear *Pilatobius recamieri* (Richters, 1911). Polar Biol. 40 (11), 2239–2252. https://doi.org/10.1007/s00300-017-2137-9.
Gąsiorek, P., Stec, D., Morek, W., Michalczyk, Ł., 2018. An integrative redescription of *Hypsibius dujardini* (Doyère, 1840), the nominal taxon for Hypsibioidea (Tardigrada: Eutardigrada). Zootaxa. 4415 (1), 45. https://doi.org/10.11646/zootaxa.4415.1.2.
Gąsiorek, P., Stec, D., Morek, W., Michalczyk, Ł., 2019. Deceptive conservatism of claws: distinct phyletic lineages concealed within Isohypsibioidea (Eutardigrada) revealed by molecular and morphological evidence. Contribut. Zool. 88 (1), 78–132. https://doi.org/10.1163/18759866-20191350.
Guidetti, R., Bertolani, R., 2001. The tardigrades of Emilia (Italy). III. Piane di Mocogno (Northern Apennines). Zool. Anz. 240 (3), 377–383. https://doi.org/10.1078/0044-5231-00045.
Guidetti, R., Bertolani, R., 2005. Tardigrade taxonomy: an updated check list of the taxa and a list of characters for their identification. Zootaxa 845 (1), 1–46. https://doi.org/10.11646/zootaxa.845.1.1.
Guidetti, R., Nelson, D.R., Bertolani, R., 1999. Ecological and faunistic studies on tardigrades in leaf litter of beach forests. Zool. Anz. 238, 215–223.
Guidetti, R., Rebecchi, L., Bertolani, R., Jönsson, K.I., Møbjerg Kristensen, R., Cesari, M., 2016. Morphological and molecular analyses on *Richtersius* (Eutardigrada) diversity reveal its new systematic position and lead to the establishment of a new genus and a new family within Macrobiotoidea. Zool. J. Linn. Soc. 178, 834–845. https://doi.org/10.1111/zoj.12428.
Kaczmarek, Ł., Michalczyk, Ł., 2017. The *Macrobiotus hufelandi* group (Tardigrada) revisited. Zootaxa 4363 (1), 101–123. https://doi.org/10.11646/zootaxa.4363.1.4.
Kaczmarek, Ł., Michalczyk, Ł., McInnes, S., 2015. Annotated zoogeography of non-marine Tardigrada. Part II: South America. Zootaxa 3923, 1–107. https://doi.org/10.11646/zootaxa.3923.1.1.
Kagoshima, H., Imura, S., Suzuki, A.C., 2013. Molecular and morphological analysis of an Antarctic tardigrade, *Acutuncus antarcticus*. J. Limnol. 72, e3.
Kalyaanamoorthy, S., Minh, B., Wong, T., von Haeseler, A., Jermiin, L.S., 2017. ModelFinder: fast model selection for accurate phylogenetic estimates. Nat. Methods 14, 587–589. https://doi.org/10.1038/nmeth.4285.
Katoh, K., Misawa, K., Kuma, K., Miyata, T., 2002. MAFFT: A novel method for rapid multiple sequence alignment based on fast Fourier transform. Nucl. Acids Res. 30, 3059–3066. https://doi.org/10.1093/nar/gkf436.
Katoh, K., Toh, H., 2008. Recent developments in the MAFFT multiple sequence alignment program. Brief. Bioinform. 9, 286–298. https://doi.org/10.1093/bib/bbn013.
Klopfstein, S., Massingham, T., Goldman, N., 2017. More on the best evolutionary rate for phylogenetic analysis. System. Biol. 66, 769–785. https://doi.org/10.1093/sysbio/syx051.
Kumar, S., Stecher, G., Tamura, K., 2016. MEGA7: molecular evolutionary genetics analysis version 7.0 for bigger datasets. Mol. Biol. Evol. 33 (7), 1870–1874. https://doi.org/10.1093/molbev/msw054.
Lanfear, R., Frandsen, P.B., Wright, A.M., Senfeld, T., Calcott, B., 2016. PartitionFinder 2: new methods for selecting partitioned models of evolution for molecular and morphological phylogenetic analyses. Mol. Biol. Evol. 34, 772–773. https://doi.org/10.1093/molbev/msw260.
Marley, N.J., McInnes, S.J., Sands, C.J., 2011. Phylum tardigrada: a re-evaluation of the parachela. Zootaxa 2819 (1), 51–64. https://doi.org/10.11646/zootaxa.2819.1.2.
McInnes, S.J., 1995. Tardigrades from Signy Island, South Orkney Islands, with particular reference to freshwater species. J. Nat. Hist. 29, 1419–1445. https://doi.org/10.1080/00222939500770601.
Michalczyk, Ł., Kaczmarek, Ł., 2013. The Tardigrada Register: a comprehensive online data repository for tardigrade taxonomy. J. Limnol. 72 (1) https://doi.org/10.4081/jlimnol.2013.s1.e22.
Miller, M.A., Pfeiffer, W., Schwartz, T., 2010. Creating the CIPRES Science Gateway for inference of large phylogenetic trees. In: 2010 Gateway Computing Environments Workshop (GCE), pp. 1–8. https://doi.org/10.1109/GCE.2010.5676129.
Minh, B.Q., Schmidt, H.A., Chernomor, O., Schrempf, D., Woodhams, M.D., von Haeseler, A., Lanfear, R., 2020. IQ-TREE 2: New models and efficient methods for phylogenetic inference in the genomic era. Mol. Biol. Evol. 37, 1530–1534. <https://doi.org/10.1093/molbev/msaa015>.
Morek, W., Stec, D., Gąsiorek, P., Schill, R.O., Kaczmarek, Ł., Michalczyk, Ł., 2016. An experimental test of eutardigrade preparation methods for light microscopy. Zool. J. Linn. Soc. 178 (4), 785–793. https://doi.org/10.1111/zoj.12457.
Morek, W., Ciosek, J.A., Michalczyk, Ł., 2020. Description of *Milnesium pentapapillatum* sp. nov., with an amendment of the diagnosis of the order Apochela and abolition of the class Apotardigrada (Tardigrada). Zool. Anz. 288, 107–117. https://doi.org/10.1016/j.jcz.2020.07.002.
Murray, J., 1907a. Scottish Tardigrada collected by the Lake Survey. Trans. R. Soc. Edinb. 45 (3), 641–668. https://doi.org/10.1017/S0080456800011777.
Murray, J., 1907b. Arctic Tardigrada, collected by Wm. S. Bruce. Trans. R. Soc. Edinb. 45 (3), 669–681. https://doi.org/10.1017/S0080456800011789.
Nelson, D.R., McGlothlin, K.L., 1993. A new species of *Hypsibius* (phylum Tardigrada) from Roan Mountain, Tennessee, USA. Trans. Am. Microsc. Soc. 140–144. https://doi.org/10.2307/3226827.
Padial, J.M., Miralles, A., De la Riva, I., Vences, M., 2010. The integrative future of taxonomy. Front. Zool. 7, 16. https://doi.org/10.1186/1742-9994-7-16.
Pilato, G., 1969. Evoluzione e nuova sistemazione degli Eutardigrada. Boll. Zool. 36, 327–345.
Pilato, G., 1981. Analisi di nuovi caratteri nello studio degli Eutardigradi. Animalia 8, 51–57.
Pilato, G., 1992. *Mixibius*, nuovo genere di Hypsibiidae (Eutardigrada). Animalia 19 (1/3), 121–125.
Pilato, G., Binda, M.G., 1997. *Acutuncus*, a new genus of Hypsibiidae (Eutardigrada). Entomol. Mitt. Zool. Mus. Hamburg. 12 (115), 159–162.
Pilato, G., Binda, M.G., 2010. Definition of families, subfamilies, genera and subgenera of the Eutardigrada, and keys to their identification. Zootaxa 2404 (1), 1–54. https://doi.org/10.11646/zootaxa.2404.1.1.
Pilato, G., Binda, M.G., Claxton, S., 2002. *Itaquascon unguiculum* and *Itaquascon cambewarrense*: two new species of eutardigrades from Australia. N. Z. J. Zool. 29 (2), 87–93. https://doi.org/10.1080/03014223.2002.9518293.
Puillandre, N., Brouillet, S., Achaz, G., 2021. ASAP: assemble species by automatic partitioning. Mol. Ecol. Resour. 21 (2), 609–620. https://doi.org/10.1111/1755-0998.13281.
Rambaut, A., 2007. FigTree, a graphical viewer of phylogenetic trees. <http://tree.bio.ed.ac.uk/software/figtree/>.
Rambaut, A., Drummond, A., Xie, D., Baele, G., Suchard, M., 2018. Posterior summarization in Bayesian phylogenetics using tracer 1.7. Syst. Biol. 67 (5), 901–904. https://doi.org/10.1093/sysbio/syy032.
Revell, L.J., 2012. Phytools: an R package for phylogenetic comparative biology (and other things). Methods Ecol. Evol. 3 (2), 217–223. https://doi.org/10.1111/j.2041-210X.2011.00169.x.
Richters, F., 1904. Vorläufiger Bericht über die antarktische Moosfauna. Verh. Dtsch. Zool. Ges. 14, 236–239.
Richters, F., 1926. Tardigrada. In: Kükenthal, W. and Krumbach, T. (Eds.). Handbuch der Zoologie, 3, 58–61.
Robotti, C., 1970. *Hypsibius (Diphascon) ramazzottii* spec. nov. e *Macrobiotus aviglianae* spec. nov. (Primo contributo alla conoscenza dei Tardigradi del Piemonte). In: Atti della Società Italiana di Scienze naturali, pp. 251–255.
Ronquist, F., Teslenko, M., van der Mark, P., Ayres, D., Darling, A., Höhna, S., Larget, B., Liu, L., Suchard, M., Huelsenbeck, J., 2012. MrBayes 3.2: Efficient Bayesian Phylogenetic Inference and Model Choice Across a Large Model Space. Syst. Biol. 61 (3), 539–542. <https://doi.org/10.1093/sysbio/sys029>.
Schill, R.O. (Ed.), 2019. Water Bears: The Biology of Tardigrades, vol. 2. Springer, pp. 1–409. <https://doi.org/10.1007/978-3-319-95702-9>.
Schultze, C.A.S., 1834. *Macrobiotus Hufelandii* animal e crustaceorum classe novum, reviviscendi post diuturnam asphixiam et aridiatem potens. Berolini Apud Carolum Curths 1834, 1–8.
Schuster, R.O., Nelson, D.R., Grigarick, A.A., Christenberry, D., 1980. Systematic criteria of the Eutardigrada. Trans. Am. Microsc. Soc. 99, 284–303. https://doi.org/10.2307/3226004.
Stec, D., Kristensen, R.M., Michalczyk, Ł., 2020b. An integrative description of *Minibiotus ioculator* sp. nov. from the Republic of South Africa with notes on *Minibiotus pentannulatus* Londoño et al. 2017 (Tardigrada: Macrobiotidae). Zool. Anz. 286, 117–134. <https://doi.org/10.1016/j.jcz.2020.03.007>.
Stec, D., Vecchi, M., Maciejowski, W., Michalczyk, Ł., 2020b. Resolving the systematics of Richtersiidae by multilocus phylogeny and an integrative redescription of the nominal species for the genus *Crenubiotus* (Tardigrada). Sci. Rep. 10, 1–20. https://doi.org/10.1038/s41598-020-75962-1.
Stec, D., Vecchi, M., Calhim, S., Michalczyk, Ł., 2021. New multilocus phylogeny reorganises the family Macrobiotidae (Eutardigrada) and unveils complex morphological evolution of the *Macrobiotus hufelandi* group. Mol. Phylogenet. Evol. 160, 106987 https://doi.org/10.1016/j.ympev.2020.106987.
Stec, D., Morek, W., 2022. Reaching the Monophyly: Re-Evaluation of the Enigmatic Species *Tenuibiotus hyperonyx* (Maucci, 1983) and the Genus *Tenuibiotus* (Eutardigrada). Animals 12. https://doi.org/10.3390/ani12030404.
Thulin, G., 1928. Über die Phylogenie und das System der Tardigraden. Hereditas 11 (2–3), 207–266. https://doi.org/10.1111/j.1601-5223.1928.tb02488.x.
Topstad, L., Guidetti, R., Majaneva, M., Ekrem, T., 2021. Multi-marker DNA metabarcoding reflects tardigrade diversity in different habitats. Genome 64 (3), 217–231.
Tumanov, D.V., 2018. *Hypsibius vaskelae*, a new species of Tardigrada (Eutardigrada, Hypsibiidae) from Russia. Zootaxa. 4399 (3), 434–442. https://doi.org/10.11646/zootaxa.4399.3.12.

Tumanov, D.V., 2020a. Integrative redescription of *Hypsibius pallidoides* Pilato et al. 2011 (Eutardigrada: Hypsibioidea) with the erection of a new genus and discussion on the phylogeny of Hypsibiidae. Eur. J. Taxon. 681, 1e37. <https://doi.org/10.5852/ejt.2020.681>.

Tumanov, D.V., 2020. Integrative description of *Mesobiotus anastasiae* sp. nov. (Eutardigrada, Macrobiotoidea) and first record of *Lobohalacarus* (Chelicerata, Trombidiformes) from the Republic of South Africa. Eur. J. Taxon. 726, 102–132. https://doi.org/10.5852/ejt.2020.726.1179.

Tumanov, D.V., 2022. End of a mystery: Integrative approach reveals the phylogenetic position of an enigmatic Antarctic tardigrade genus *Ramajendas* (Tardigrada, Eutardigrada). Zool. Scr. 51, 217–231. https://doi.org/10.1111/zsc.12521.

Utsugi, K., Ohyama, Y. 1989. Antarctic tardigrada. In: Proceedings of the NIPR Symposium on Polar Biology. 2: 190–197.

Vecchi, M., Bruneaux, M., 2021. Concatipede: an R package to concatenate fasta sequences easily. <http://doi.org/10.5281/zenodo.5130604>.

Van Rompu, E.A., De Smet, W.H., 1991. Contribution to the fresh water Tardigrada from Barentsøya, Svalbard (78 30'N). Fauna Norvegica: seria A: Norwegian fauna except entomology and ornithology. Oslo 12, 29–39.

Vecchi, M., Ferrari, C., Stec, D., Calhim, S., 2022. Desiccation risk favours prevalence and diversity of tardigrade communities and influences their trophic structure in alpine ephemeral rock pools. Hydrobiologia 849, 1995–2007. https://doi.org/10.1007/s10750-022-04820-0.

Zhang, J., Kapli, P., Pavlidis, P., Stamatakis, A., 2013. A general species delimitation method with applications to phylogenetic placements. Bioinformatics. 29 (22), 2869–2876. https://doi.org/10.1093/bioinformatics/btt499.

Zawierucha, K., Buda, J., Jaromerska, T.N., Janko, K., Gąsiorek, P., 2020. Integrative approach reveals new species of water bears (*Pilatobius*, *Grevenius*, and *Acutuncus*) from Arctic cryoconite holes, with the discovery of hidden lineages of *Hypsibius*. Zool. Anz. 289, 141–165. https://doi.org/10.1016/j.jcz.2020.09.004.

Zawierucha, K., Stec, D., Dearden, P.K., Shain, D.H., 2022. Two new tardigrade genera from New Zealand's southern alp glaciers display morphological stasis and parallel evolution. Mol. Phylogenet. Evol. 107634 (178), 1–14. https://doi.org/10.1016/j.ympev.2022.107634.